# Theory of Fluorescence Induction in Photosystem II: Derivation of Analytical Expressions in a Model Including Exciton–Radical-Pair Equilibrium and Restricted Energy Transfer Between Photosynthetic Units

Jérôme Lavergne* and Hans-Wilhelm Trissl[‡]

*Institut de Biologie Physico-Chimique, 75005 Paris, France; and [‡]Abt. Biophysik, Fachbereich Biologie/Chemie, Universität Osnabrück, Osnabrück, Germany

ABSTRACT   The theoretical relationships between the fluorescence and photochemical yields of PS II and the fraction of open reaction centers are examined in a general model endowed with the following features: i) a homogeneous, infinite PS II domain; ii) exciton–radical-pair equilibrium; and iii) different rates of exciton transfer between core and peripheral antenna beds. Simple analytical relations are derived for the yields and their time courses in induction experiments. The introduction of the exciton–radical-pair equilibrium, for both the open and closed states of the trap, is shown to be equivalent to an irreversible trapping scheme with modified parameters. Variation of the interunit transfer rate allows continuous modulation from the case of separated units to the pure lake model. Broadly used relations for estimating the relative amount of reaction centers from the complementary area of the fluorescence kinetics or the photochemical yield from fluorescence levels are examined in this framework. Their dependence on parameters controlling exciton decay is discussed, allowing assessment of their range of applicability. An experimental induction curve is analyzed, with a discussion of its decomposition into $\alpha$ and $\beta$ contributions. The sigmoidicity of the induction kinetics is characterized by a single parameter $J$ related to Joliot's $p$, which is shown to depend on both the connectivity of the photosynthetic units and reaction center parameters. On the other hand, the relation between $J$ and the extreme fluorescence levels (or the deviation from the linear Stern–Volmer dependence of $1/\Phi_f$ on the fraction of open traps) is controlled only by antenna connectivity. Experimental data are consistent with a model of connected units for PS II$_\alpha$, intermediate between the pure lake model of unrestricted exciton transfer and the isolated units model.

## INTRODUCTION

The yield of the chlorophyll fluorescence emitted by chloroplasts is a sensitive measure of the redox state of the PS II reaction center. It was originally shown by Duysens and Sweers (1963) that the reduced state of the primary quinone acceptor $Q_A$ (closed center) induces a high fluorescence yield, whereas the oxidized $Q_A$ (open center) is a quenching

state. The kinetics of the fluorescence rise from the open state (minimum yield $F_o$) to the closed state (maximal yield $F_m$) that are observed during a continuous illumination is called fluorescence induction and has been widely used as a convenient tool for studying PS II (for reviews, see Lavorel and Etienne, 1977; Govindjee and Jursinic, 1979; Lavorel et al., 1986; van Gorkom, 1986). Throughout this text, "induction kinetics" will refer to experimental conditions where electron transfer is blocked beyond $Q_A^-$, using for instance the inhibitor DCMU. Typical information derived from the induction curves concerns the antenna size, the content of active PS II centers, and the heterogeneity of PS II.

The concept of exciton-radical pair equilibrium (or reversible radical pair) has emerged from fast spectroscopic techniques suggesting that rapid equilibration of the exciton occurs among all pigments of PS II (antenna + RC) and that the exciton decay is significantly influenced by the reversibility of the primary charge separation (van Gorkom, 1985; Schatz et al., 1988; Leibl et al., 1989; see Dau (1994) for a review). In a recent paper (Trissl et al., 1993; see also the accompanying comment paper, Holzwarth, 1993), the problem of exciton trapping in a simple lake model (PS II

centers sharing excitation from an infinitely large pigment bed; Robinson, 1967) was analyzed, introducing explicitly the equilibrium between the exciton and the radical pair created in a reaction center by photochemical trapping. Results from this study led the authors to reexamine critically the significance of parameters (complementary area and curvature of the induction kinetics) broadly used in experimental work.

The purpose of the present paper is twofold. First, we shall analyze the mathematical methods that can be used for dealing with such problems. It will be shown that the numerical integration used by Trissl et al. (1993) can be replaced by an exact analytical derivation that can be applied to a variety of models featuring both exciton–radical-pair equilibrium and limited antenna connectivity, even for heterogeneous antenna systems. The outcome of this section (which may be skipped by readers who are not interested primarily in mathematical aspects) consists of simple general expressions for the fluorescence and photochemical yields as functions of the amount of open traps and also of a simple general kinetic law for the induction curves. This will lead us to reexamine and to qualify some of the conclusions expressed by Trissl et al. (1993) or Holzwarth (1993).

Unfortunately, some errors were present in Trissl et al. (1993) (see Erratum, Biophys. J. **65**, 982–983 (1993)): (i) In data set 3 of Table 1, $\Phi_p$ and $F_o$ were calculated with $k_r = 0$, whereas $F_m$, $F_v$ and $F_a$ used $k_r = (1.3 \text{ ns})^{-1}$. The consequence was an apparent failure of the relation $\phi_p \cdot F_a/F_v = 1$, which is in fact fully valid, as will be shown. (ii) Another error was noted by Falkowski et al. (1994), i.e., computing $(F_v/F_m) \cdot \Phi_p$ instead of $(F_v/F_m)/\phi_p$ (p. 983).

## MATHEMATICAL ASPECTS

### Analytical derivation for the exciton-radical pair equilibrium model

The basic features of the model treated by Trissl et al. (1993) were the following: i) Pure lake model: the reaction centers are embedded in a common antenna system of infinite size, and the diffusion of the exciton among all pigments (antenna + RC) is assumed to be fast with respect to reactions at the reaction center, so that the exciton density is uniform. ii) Exciton–radical-pair equilibrium: explicit rate constants for the trapping and detrapping of the exciton are taken into account for both open and closed states of the center. iii) A transient quenching process is taken into account, namely, quenching by the oxidized state (P-680$^+$) of the primary photochemical donor.

In the present treatment, we shall drop point iii) above, because the effect of this transient quenching is in fact totally negligible under the experimental conditions used for studying fluorescence induction in the millisecond-to-second time range. Indeed, this process has characteristic lifetimes on the 100-ns scale (reduction of P-680$^+$ by tyrosine $Y_Z$ when the oxygen-evolving enzyme has not been inactivated). Thus, the quenching by P-680$^+$ may be ignored whenever the exciton

creation rate is below, say, 1 ($\mu$s center)$^{-1}$, which is usually the case in induction experiments corresponding to $t_{1/2}$ of 1–100 ms. This also applies to the treatment used by Trissl et al. (1993) that simulated the induction by a train of infinitely (in the limit) weak Dirac light pulses, spaced so that the reactions caused by each pulse were totally relaxed before the next pulse occurred. However, when the induction is driven by submicrosecond intense light pulses, this and other transient quenching processes are of important consequence, and failure to recognize this may have been, as argued below, the origin of some confusion in the literature.

Neglecting the quenching by P-680$^+$ leads to a system of differential equations describing the exciton decay with first-order or pseudo-first-order rate constants, namely, $k_1$ for decay from the antenna (including the radiative pathway; $k_{rad}$); $q k_t^{ox}$ and $k_{-1}^{ox}$ for, respectively, trapping and detrapping by an open center, $(1 - q)k_t^{red}$ and $k_{-1}^{red}$ for trapping and detrapping by a closed center, $k_2$ and $k_d^{ox}$ for, respectively, radical pair decay in an open center through stabilization of charge (reduction of $Q_A$) or nonradiative losses; and $k_d^{red}$ for nonradiative losses from the radical pair in a closed center. We denote by $q$ the fraction of open centers. Because $q$ does not vary during an infinitesimal flash, it appears as a constant in the differential equations, and it has been directly associated with the second-order rate constants for trapping, expressed as the pseudo-first-order constants $q k_t^{ox}$ and $(1 - q)k_t^{red}$. It should be kept in mind that the rate constants $k_t^{ox}$ and $k_t^{red}$ describe the effective trapping of excitons *from the antenna as a whole*. If the excitation is homogeneously spread over all chlorophylls (including the reaction center), the exciton is found on the center with the probability $1/(N + 1) \approx 1/N$ (where $N$ is the antenna size). If a spectral heterogeneity among the antenna pigments is taken into account, $N$ may be replaced by an effective antenna size, $N_{eff}$ (Trissl, 1993; for a discussion of the approximations involved, see Laible et al., 1994). Thus, these two global rate constants are equal to the corresponding intrinsic parameters for the naked center divided by $N$. This reaction scheme, described in Fig. 1, assumes that charge stabilization is achieved on reduction of $Q_A$ (with the rate constant $k_2$). Although this assumption is correct on a nanosecond time scale, it probably is not on a longer scale, because a significant recombination of $Q_A^-$ is
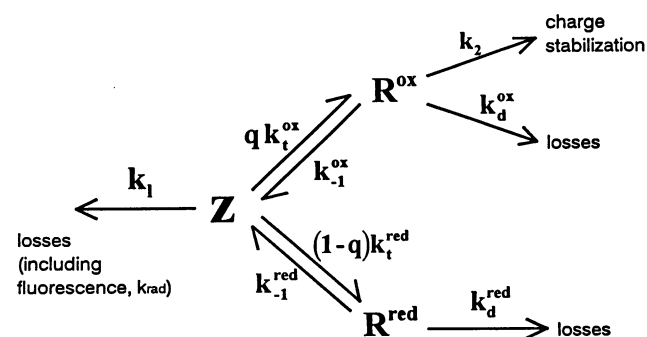


FIGURE 1   Kinetic scheme of the exciton decay routes assuming exciton radical pair equilibrium in the case of a lake model.

expected to occur as long as a positive charge is present on P-680$^+$ or on the secondary donor $Y_Z^+$. This is probably one of the causes of the photochemical misses (5–9%) accounting for the damping of the Kok cycle under a train of saturating short flashes. For simplicity, we did not implement this additional loss pathway in out treatment, but we indicate below how this can be done. The scheme of Fig. 1 leads to the following system:

$$\frac{dz}{dt} = -(k_1 + qk_t^{ox} + (1 - q)k_t^{red})z$$

$$+ k_{-1}^{ox} R^{ox} + k_{-1}^{red} R^{red}, \quad (1a)$$

$$\frac{dR^{ox}}{dt} = -(k_{-1}^{ox} + k_2 + k_d^{ox})R^{ox} + qk_t^{ox} z, \quad (1b)$$

$$\frac{dR^{red}}{dt} = -(k_{-1}^{red} + k_d^{red})R^{red} + (1 - q)k_t^{red} z, \quad (1c)$$

where $z$, $R^{ox}$, and $R^{red}$ stand for the concentrations of exciton, radical pair in open centers, and radical pair in closed centers, respectively. This system of linear differential equations can be solved analytically. This need not be done, however, if one is interested in the overall yields rather than in the detailed kinetics of exciton decay. It suffices then to integrate the above expressions from $t = 0$ to $t = \infty$; thus (the initial concentration of excitons is denoted by $z_0$):

$$\int_0^\infty \frac{dz}{dt} dt = -z_0 = -(k_t + qk_t^{ox} + (1 - q)k_t^{red})$$

$$\int_0^\infty z\,dt + k_{-1}^{ox} \int_0^\infty R^{ox}\,dt + k_{-1}^{red} \int_0^\infty R^{red}\,dt, \quad (2a)$$

$$\int_0^\infty \frac{dR^{ox}}{dt} dt = 0 = -(k_{-1}^{ox} + k_2 + k_d^{ox})$$

$$\int_0^\infty R^{ox}\,dt + qk_t^{ox} \int_0^\infty z\,dt, \quad (2b)$$

$$\int_0^\infty \frac{dR^{red}}{dt} dt = 0 = -(k_{-1}^{red} + k_d^{red})$$

$$\int_0^\infty R^{red}\,dt + (1 - q)k_t^{red} \int_0^\infty z\,dt. \quad (2c)$$

We now have a system of linear algebraic equations with the three integrals as unknowns. Solving this system gives

$$\int_0^\infty z\,dt = \frac{z_0}{q(\alpha_p + \alpha_d - \beta) + \beta + k_1}, \quad (3a)$$

$$\int_0^\infty R^{ox}\,dt = q \frac{\alpha_p}{k_2} \int_0^\infty z\,dt, \quad (3b)$$

$$\int_0^\infty R^{red}\,dt = (1 - q)\frac{\beta}{k_d^{red}} \int_0^\infty z\,dt, \quad (3c)$$

where

$$\alpha_p = \frac{k_t^{ox} k_2}{k_{-1}^{ox} + k_2 + k_d^{ox}}, \quad (4a)$$

$$\alpha_d = \frac{k_t^{ox} k_d^{ox}}{k_{-1}^{ox} + k_2 + k_d^{ox}}, \quad (4b)$$

$$\beta = \frac{k_t^{red} k_d^{red}}{k_{-1}^{red} + k_d^{red}}. \quad (4c)$$

We then obtain the yields for fluorescence ($\Phi_f$) and photochemistry ($\Phi_p$):

$$\Phi_f(q) = \frac{k_{rad}}{z_0} \int_0^\infty z\,dt = \frac{k_{rad}}{\beta + k_1 + (\alpha_p + \alpha_d - \beta)q}, \quad (5a)$$

$$\Phi_p(q) = \frac{k_2}{z_0} \int_0^\infty R^{ox}\,dt$$

$$(5b)$$

$$= q \frac{\alpha_p}{\beta + k_1 + (\alpha_p + \alpha_d - \beta)q}.$$

As mentioned above, this treatment does not explicitly take into account the additional losses occurring after $Q_A^-$ formation through recombination with P-680$^+$ before the oxidized equivalent is stabilized on the donor side. This decay pathway can be introduced easily at this step. If we express its yield by $1 - \varphi$ (thus, $\varphi \approx 0.95$ denotes the stabilization yield of $Q_A^-$, then Eq. 5b (and further expressions involving the photochemical yield, such as Eq. 10 below) should be multiplied by $\varphi$.

It is convenient to note that Eqs. 5 have the general form

$$\Phi_f(q) = \frac{B + Cq}{1 + Jq}, \quad (6a)$$

$$\Phi_p(q) = \frac{Aq}{1 + Jq}, \quad (6b)$$

with, in the present case,

$$J = \frac{\alpha_p + \alpha_d - \beta}{\beta + k_1}, \quad (7a)$$

$$A = \frac{\alpha_p}{\beta + k_1}, \quad (7b)$$

$$B = \frac{k_{rad}}{\beta + k_1}, \quad (7c)$$

$$C = 0. \quad (7d)$$

When all centers are open ($q = 1$), the fluorescence yield

is minimum and the photochemical yield maximum:

$$\Phi_o = \Phi_f(1) = \frac{k_{rad}}{\alpha_p + \alpha_d + k_1}, \tag{8a}$$

$$\Phi_p(1) = \frac{\alpha_p}{\alpha_p + \alpha_d + k_1}. \tag{8b}$$

When all centers are closed, the photochemical yield is zero and the fluorescence yield maximum:

$$\Phi_m = \Phi_f(0) = \frac{k_{rad}}{\beta + k_1}, \tag{8c}$$

so that

$$\frac{\Phi_m}{\Phi_o} = \frac{\alpha_p + \alpha_d + k_1}{\beta + k_1}. \tag{8d}$$

Expressions of the form of Eqs. 6 were previously derived in a model that did not take an exciton–radical-pair equilibrium explicitly into account (Lavergne and Leci, 1993). As those authors noted, these expressions are also of the same form as those originally derived by Joliot and Joliot (1964). The parameter $J$ is related to Joliot's connection parameter $p$ by

$$J = \frac{p}{1 - p}. \tag{9}$$

Following this earlier work, we obtain an analytical solution for the fluorescence induction kinetics, noting that

$$-\frac{dq}{dt} = I\,\Phi_p(q), \tag{10}$$

where $I$ denotes the rate of exciton creation (per PS II center). Thus,

$$dt = -\frac{1}{I\Phi_p(1)(1 + J)}\left(\frac{dq}{q} + J dq\right), \tag{11}$$

$$t = \frac{J(1 - q) - \ln q}{I\Phi_p(1)(1 + J)}, \tag{12}$$

using the initial condition $q = 1$ for $t = 0$. The fluorescence induction kinetics are obtained by use of $q$ as a parameter, by combining Eqs. 12 and 6b. As expected, the curves computed from the above expressions (see Fig. 6; the time scale was normalized to hits per PSU by taking $I = 1$) are in perfect agreement with the results obtained from numerical integration by Trissl et al. (1993).

From the form of Eqs. 5, it may be realized that the exciton–radical-pair model turns out to be homologous to a model with irreversible decay and trapping processes, with effective rate constants indicated in Fig. 2. It should be kept in mind that this equivalence holds for the calculation of overall yields but would not apply to that of the decay kinetics. Within this scope, this brings up a major simplification, as we can replace the exciton–radical-pair equilibrium model by the simple branched decay of Fig. 2. A similar conclusion was reached by Dau (1994), who pointed out the
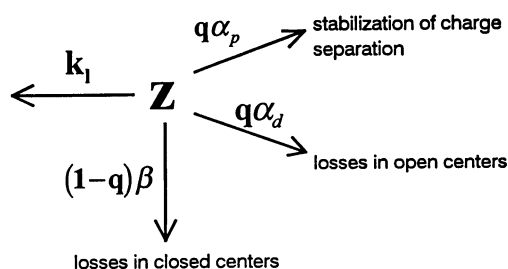


FIGURE 2  Irreversible branched decay scheme equivalent to the scheme of Fig. 1. $\alpha_p$, $\alpha_d$, and $\beta$ are defined in Eq. 4 a–c.

formal homology of this problem with Butler's bipartite model (Butler and Kitajima, 1975; Butler, 1978).

## Random walk in a network of states

The method described above consisted of writing the appropriate set of differential equations for the exciton decay, then integrating them to obtain yields. A very useful shortcut can be found for dealing with such problems that may save much intricate algebra. Instead of considering concentrations of various species (excitons and radical pairs), we can treat the problem as a random walk where the excitation may adopt different and mutually exclusive states. This viewpoint is justified because, as emphasized above, we are dealing with a linear problem in which these various states do not interact with one another (no exciton collision with another exciton or radical pair). We can thus transform the kinetic scheme into a random-walk network in which rate constants are replaced by hopping probabilities between states, as shown in Fig. 3. These probabilities are of the form

$$P_{ij} = \frac{k_{ij}}{\sum_{l=0}^{3} k_{ij}}, \tag{13}$$

where the $k_{ij}$ may be read from Fig. 1. State $A_1$ stands for the antenna exciton and states $A_2$ and $A_3$ stand for the radical pair in an open or a closed center, respectively. The excitation is initially created in the antenna (state $A_1$). From this starting point, an infinity of histories is possible for the random walk [such as $(A_1A_2)$, $(A_1A_3A_1A_2)$], where the last state indicates where deactivation eventually occurs. Let us denote by



FIGURE 3  Equivalent random-walk network and transition probabilities for the scheme of Fig. 1.

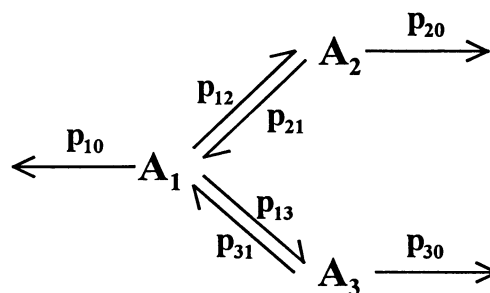$P(i, j)$ the summed probability for all histories starting at $i$ and ending at $j$. We begin with $P(1, 1)$ for which the first step contribution is the direct decay from $A_1$ (probability $p_{10}$); the next contributions will require three steps: jumping to $A_2$, jumping back to $A_1$, and decaying in $A_1(p_{12}p_{21}p_{10})$ and the equivalent process with $A_3(p_{13}p_{31}p_{10})$. Instead of summing the infinite series of terms, we may notice that, when the exciton is back on $A_1$, it still has the probability $P(1, 1)$ to decay eventually in $A_1$. Thus, one has

$$P(1, 1) = p_{10} + p_{12}p_{21}P(1, 1) + p_{13}p_{31}P(1, 1), \quad (14)$$

$$P(1, 1) = \frac{p_{10}}{1 - p_{12}p_{21} - p_{13}p_{31}}. \quad (15)$$

Similarly,

$$P(1, 2) = p_{12}p_{20} + p_{12}p_{21}P(1, 2) + p_{13}p_{31}P(1, 2), \quad (16)$$

$$P(1, 2) = \frac{p_{12}p_{20}}{1 - p_{12}p_{21} - p_{13}p_{31}}. \quad (17)$$

Then the fluorescence and photochemical yields are

$$\Phi_f = \frac{k_{rad}}{k_l}P(1, 1), \quad (18a)$$

$$\Phi_p = \frac{k_2}{k_2 + k_d^{ox}}P(1, 2), \quad (18b)$$

which is equivalent to Eqs. 5 when one is expressing the $p_{ij}$ in terms of $k_{ij}$, using Eq. 13. This treatment thus gives the yields directly, with no need for solving any linear system.

## General model with heterogenous antenna domains

The random-walk treatment proves to be especially useful when one is dealing with more complex models in which antenna heterogeneity is considered in addition to the exciton-radical-pair equilibrium. We illustrate this with the example pictured in Fig. 4. Here, we consider a peripheral antenna $A$, containing no reaction centers but exchanging excitons with photosynthetic units $U$, composed of a core antenna and one reaction center. For generality, we also allow direct exciton transfer between the units $U$. This assumption is not necessarily meant to portray a realistic physical situation, but the general expressions that we shall derive will be readily applicable to subcases in which only $A$–$U$ transfers occur, or only $U$–$U$ transfers (deleting $A$ in this case). As will be shown, the final expressions have a form similar to Eqs. 6 and 12, warranting a broad generality in the subsequent discussion.

In the scheme of Fig. 4, the units $U$ are labeled ox or red, depending on whether the state of the center is open or closed. The fraction of $U^{ox}$ is $q$ and that of $U^{red}$ is $(1 - q)$, and these quantities are included in the pseudo-first-order rate constants concerning transfer toward $U^{ox}$ or $U^{red}$. The initial distribution of excitons between $A$ and $U$ depends on the relative cross sections of these antennas. We denote by $a$ the
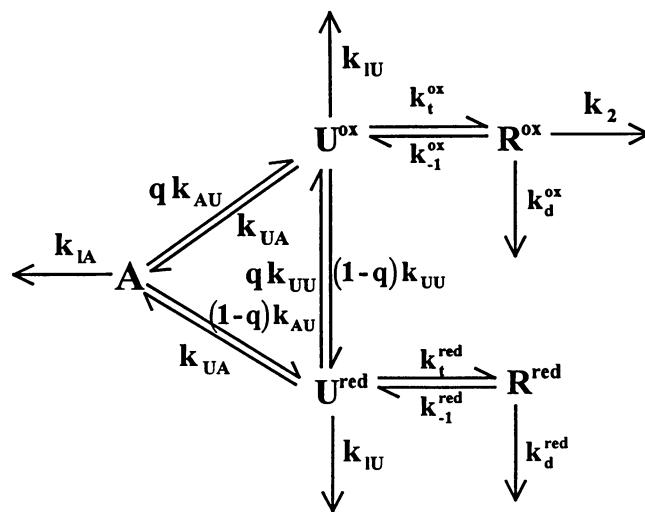


FIGURE 4 Random-walk network for a heterogeneous antenna system consisting of a peripheral antenna $A$, containing no reaction centers but exchanging excitons with photosynthetic units $U$ composed of a core antenna and one reaction center. The trapping in $U$ occurs according to the exciton-radical-pair equilibrium model.

fraction of photons absorbed by $A$; thus $(1 - a)$ is absorbed by $U$, with $(1 - a)q$ in open units and $(1 - a)(1 - q)$ in closed units.

As mentioned above, this scheme can be simplified by use of the irreversible branched decay equivalent to the exciton-radical-pair model. This gives the network of Fig. 5. The scheme directly features transition probabilities that we deduce from rate constants by using Eq. 13. The corresponding rate constants may be read from Fig. 3, except $k_{20}$ and $k_{30}$, which are now the effective rate constants resulting from the above simplification:

$$k_{10} = k_1^A, \quad (19a)$$

$$k_{20} = \alpha_p + \alpha_d + k_1^U, \quad (19b)$$

$$k_{30} = \beta + k_1^U. \quad (19c)$$

The expressions for the $p_{ij}$ are summarized in Table 1. As before, we denote by $P(i, j)$ the total probability that an exciton starting from $A_i$ eventually has to decay in $A_j$. Clearly, this probability does not depend on the previous history of
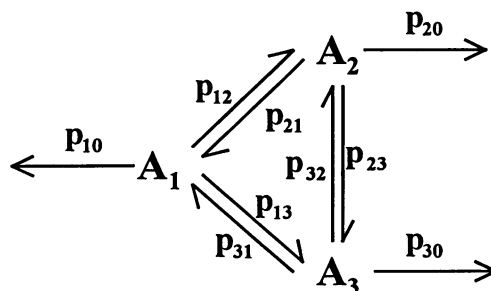


FIGURE 5 Probability network corresponding to Fig. 4 using the irreversible branched decay of Fig. 2, equivalent to the exciton-radical-pair model.

**TABLE 1 Transition probabilities for the network of Fig. 5**

$$p_{10} = \frac{k_1^A}{k_{AU} + k_1^A}, \qquad p_{12} = \frac{q k_{AU}}{k_{AU} + k_1^A}, \qquad p_{13} = \frac{(1-q)k_{AU}}{k_{AU} + k_1^A},$$

$$p_{20} = \frac{\alpha_p + \alpha_d + k_1^U}{\alpha_p + \alpha_d + k_1^U + (1-q)k_{UU} + k_{UA}}, \qquad p_{21} = \frac{k_{UA}}{\alpha_p + \alpha_d + k_1^U + (1-q)k_{UU} + k_{UA}}, \qquad p_{23} = \frac{(1-q)k_{UU}}{\alpha_p + \alpha_d + k_1^U + (1-q)k_{UU} + k_{UA}},$$

$$p_{30} = \frac{\beta + k_1^U}{\beta + k_1^U + q k_{UU} + k_{UA}}, \qquad p_{31} = \frac{k_{UA}}{\beta + k_1^U + q k_{UU} + k_{UA}}, \qquad p_{32} = \frac{q k_{UU}}{\beta + k_1^U + q k_{UU} + k_{UA}}$$

the exciton, preceding the arbitrary "start" at $A_i$. Thus, for the various probabilities $P(i, 2)$ of decay in an open center $(A_2)$, we can write the system

$$P(2, 2) = p_{20} + p_{23}P(3, 2) + p_{21}P(1, 2), \qquad (20a)$$

$$P(3, 2) = p_{32}P(2, 2) + p_{31}P(1, 2), \qquad (20b)$$

$$P(1, 2) = p_{12}P(2, 2) + p_{13}P(3, 2), \qquad (20c)$$

where, for instance, the Eq. 20a means that the total probability to start at $A_2$ and eventually to decay at $A_2$ is the sum of the probabilities to decay right away at $A_2$, to hop to $A_3$, and eventually to decay in $A_2$, *starting from* $A_3$, and to hop to $A_1$ and eventually to decay in $A_2$, *starting from* $A_1$. Solving this linear system gives

$$P(2, 2) = p_{20} \frac{1 - p_{13}p_{31}}{D}, \qquad (21a)$$

$$P(3, 2) = p_{20} \frac{p_{32} + p_{12}p_{31}}{D}, \qquad (21b)$$

$$P(1, 2) = p_{20} \frac{p_{12} + p_{13}p_{32}}{D}, \qquad (21c)$$

with

$$D = 1 - (p_{13}p_{32}p_{21} + p_{12}p_{23}p_{31} + p_{12}p_{21} + p_{13}p_{31} + p_{23}p_{32}). \qquad (21d)$$

From these expressions, one can obtain the photochemical yield as follows. The total yield of decay from $A_2$ is

$$\Phi_2 = aP(1, 2) + (1 - a)[qP(2, 2) + (1 - q)P(3, 2)], \qquad (22)$$

which takes into account the initial distribution of excitons. Replacing the $p_{ij}$ by their values in terms of rate constants, one gets (skipping elementary but lengthy algebra)

$$\Phi_2 = k_{20}q \frac{(k_{UA} + k_{UU} + k_{30})(k_{AU} + k_{10} - ak_{10})}{D'}, \qquad (23a)$$

where

$$D' = (k_{UA} + k_{UU} + k_{20})(k_{UA}\,k_{10} + k_{AU}\,k_{30} + k_{10}\,k_{30})$$
$$+ (k_{20} - k_{30})(k_{AU}\,k_{UA} + k_{UU}\,k_{AU} + k_{UU}\,k_{10})q. \qquad (23b)$$

The photochemical yield is then obtained by

$$\Phi_p = \frac{\alpha_p}{k_{20}} \Phi_2. \qquad (24)$$

A few more steps are required to obtain the fluorescence yield. Consistent with Eq. 22, we denote by $\Phi_i$ the yield for total decay from $A_i$. Then

$$\Phi_f = \frac{k_{rad}^A}{k_{10}} \Phi_1 + \frac{k_{rad}^U}{k_{20}} \Phi_2 + \frac{k_{rad}^U}{k_{30}} \Phi_3, \qquad (25)$$

where a superscript accounts for a possible different $k_{rad}$ from the two types of antenna. We have already calculated $\Phi_2$. The problem of obtaining $\Phi_3$ is entirely homologous and amounts to interchanging indexes 2 and 3 or, for the rate constants, substituting $k_{20}$ for $k_{30}$ and $q$ for $(1 - q)$. This leaves the denominator (Eq. 23b) unchanged and gives

$$\Phi_3 = k_{30}(1 - q) \qquad (26)$$
$$\frac{(k_{UA} + k_{UU} + k_{20})(k_{AU} + k_{10} - ak_{10})}{D'}.$$

$\Phi_1$ is now easily obtained as $1 - \Phi_2 - \Phi_3$ (because the exciton has to decay from one of the three domains). Thus, using Eqs. 23b and 25–26, we finally obtain

$$\Phi_f(q) = \frac{X + Yq}{D'}, \qquad (27a)$$

with

$$X = (k_{UA} + k_{UU} + k_{20})[k_{rad}^A (k_{UA} + ak_{30}) \qquad (27b)$$
$$+ k_{rad}^U (k_{AU} + k_{10} - ak_{10})],$$

$$Y = (k_{20} - k_{30})[k_{rad}^A(a(k_{UA} + k_{UU}) - k_{UA}) \qquad (27c)$$
$$- k_{rad}^U (k_{AU} + k_{10} - ak_{10})].$$

Although they are complex in terms of elementary rate constants, the expressions for $\Phi_p$ and $\Phi_f$ keep the simple hyperbolic dependence on $q$ shown in Eqs. 6, with now

$$J = \frac{(k_{20} - k_{30})(k_{AU}k_{UA} + k_{UU}k_{AU} + k_{UU}k_{10})}{(k_{UA} + k_{UU} + k_{20})(k_{UA}k_{10} + k_{AU}k_{30} + k_{10}k_{30})}, \qquad (28a)$$

$$A = \alpha_p \frac{(k_{UA} + k_{UU} + k_{30})(k_{AU} + k_{10} - ak_{10})}{(k_{UA} + k_{UU} + k_{20})(k_{UA}\,k_{10} + k_{AU}\,k_{30} + k_{10}\,k_{30})}, \qquad (28b)$$

$$B = \frac{k_{rad}^A(k_{UA} + ak_{30}) + k_{rad}^U (k_{AU} + k_{10} - ak_{10})}{k_{UA}k_{10} + k_{AU}k_{30} + k_{10}k_{30}}, \quad (28c)$$

$$C = (k_{20} - k_{30})[k_{rad}^A(a(k_{UA} + k_{UU})$$
$$\frac{- k_{UA}) - k_{rad}^U (k_{AU} + k_{10} - ak_{10})]}{(k_{UA} + k_{UU} + k_{20})(k_{UA} k_{10} + k_{AU} k_{30} + k_{10} k_{30})}. \quad (28d)$$

### First subcase: funneling model

In the current view of the organization of the PS II reaction center complexes and their light-harvesting chlorophyll proteins, the reaction center is immediately surrounded by core antenna proteins including mostly chlorophyll-*a*, whereas LHC-II, richer in chlorophyll-*b*, is located peripherally. It is thus likely that RC–RC exciton transfers must occur via the LHC II rather than through core–core transfers (see, however, the dimeric PS II models of Peter and Thornber, 1991 or Dainese and Bassi, 1991). This is essentially the case treated by Butler (1978) in his tripartite model (with some differences concerning the properties of the RCs). This situation can be modeled easily from the foregoing by taking $k_{UU} = 0$. The yields keep the same form as in Eqs. 6, whereas Eqs. 28 become

$$J = \frac{k_{AU}k_{UA}(k_{20} - k_{30})}{(k_{UA} + k_{20})(k_{UA} k_{10} + k_{AU}k_{30} + k_{10}k_{30})}, \quad (29a)$$

$$A = \alpha_p \frac{(k_{UA} + k_{30})(k_{AU} + k_{10} - ak_{10})}{(k_{UA} + k_{20})(k_{UA}k_{10} + k_{AU} k_{30} + k_{10} k_{30})}, \quad (29b)$$

$$B = \frac{k_{rad}^A (k_{UA} + ak_{30}) + k_{rad}^U (k_{AU} + k_{10} - ak_{10})}{k_{UA} k_{10} + k_{AU} k_{30} + k_{10} k_{30}}, \quad (29c)$$

$$C = \frac{(k_{20} - k_{30})[k_{rad}^A k_{UA}(a - 1) - k_{rad}^U (k_{AU} + k_{10} - ak_{10})]}{(k_{UA} + k_{20})(k_{UA} k_{10} + k_{AU} k_{30} + k_{10} k_{30})}. \quad (29d)$$

### Second subcase: connected units

Although it is justified from a realistic point of view, the foregoing model remains difficult to handle because of its many parameters. To discuss the respective effects of rate constants related to the RC and to the connectivity of the antenna, we now consider another simple model that consists of deleting the peripheral antenna $A$ altogether ($a = k_{AU} = k_{UA} = 0$) but allowing the $U$–$U$ transfer. In fact, the funneling effect in the PS II antenna that is due to the longer-wavelength pigments in the core antenna is relatively minor (Trissl, 1993), so that one does not lose a crucial parameter by considering a homogeneous antenna. Then a finite rate constant $k_{UU}$ accounts for imperfect connectivity between PS II units. The limiting cases of zero (isolated units) or infinite connectivity (lake model) are easily obtained by varying $k_{UU}$ accordingly. Equations 28 now become (we write $k_{rad}^U = k_{rad}$)

$$J = \frac{k_{UU} (k_{20} - k_{30})}{k_{30}(k_{UU} + k_{20})}$$

$$(30a)$$

$$= \frac{k_{UU}(\alpha_p + \alpha_d - \beta)}{(\beta + k_1)(k_{UU} + \alpha_p + \alpha_d + k_1)},$$

$$A = \frac{\alpha_p(k_{UU} + k_{30})}{k_{30}(k_{UU} + k_{20})}$$

$$(30b)$$

$$= \frac{\alpha_p(k_{UU} + \beta + k_1)}{(\beta + k_1)(k_{UU} + \alpha_p + \alpha_d + k_1)},$$

$$B = \frac{k_{rad}}{k_{30}} = \frac{k_{rad}}{(\beta + k_1)}, \quad (30c)$$

$$C = \frac{k_{rad}(k_{30} - k_{20})}{k_{30}(k_{UU} + k_{20})}$$

$$(30d)$$

$$= - \frac{k_{rad}(\alpha_p + \alpha_d - \beta)}{(\beta + k_1)(k_{UU} + \alpha_p + \alpha_d + k_1)}.$$

The extreme fluorescence levels $\Phi_o$ and $\Phi_m$ and the photochemical yield $\Phi_p(1)$ are the same as derived for the lake model (Eqs. 8). These quantities do not depend on the rate of interunit transfer $k_{UU}$ (nor on $J$) and thus remain the same irrespective of whether the connectivity is finite (connected units), infinite (lake), or zero (isolated units).

Fluorescence induction curves according to the connected units model are shown in Fig. 6 (*a*) for various values of $k_{UU}$ (the corresponding values of $J$ are indicated in the caption). The other parameters are those estimated for $\alpha$ centers by Roelofs et al. (1992). The rate constant $k_d^{red}$ (losses on the closed center) plays an important role because it substantially controls the maximal fluorescence yield $\Phi_m$ (and also the sigmoidicity parameter $J$, as further discussed below). The requirement for a significant decay path on the closed center was emphasized by Duysens (1979). An alternative possibility accounting for the experimental range of the $\Phi_m/\Phi_o$ ratio would be to assume a larger rate for decay in the antenna ($k_1$), implying a low photochemical yield of PS II (of ~0.7 instead of 0.9), as was proposed by Thielen and van Gorkom (1981). However, this view is hardly consistent with the current data for the decay rates in PS II and also with other estimates of the quantum yield (Joliot et al., 1968).

### General properties of the yield expressions

In spite of the complexity of our general model (from which we derived the two simpler subcases described above), which allows us to take into account both exciton–radical-pair equilibrium at the level of the RC and imperfect transfer among different antenna beds, the expressions relating the yields $\Phi_p$ and $\Phi_f$ to $q$ take the very simple hyperbolic forms of Eqs. 6. We would like now to describe some general consequences of these expressions.

### Joliot's equation

With the definitions $\Phi_o = \Phi_f(1)$, $\Phi_m = \Phi_f(0)$, $\Phi_v(q) = \Phi_f(q) - \Phi_o$, and $\Phi_v^m = \Phi_v(0) = \Phi_m - \Phi_o$, we can rewrite Eq. 6a as
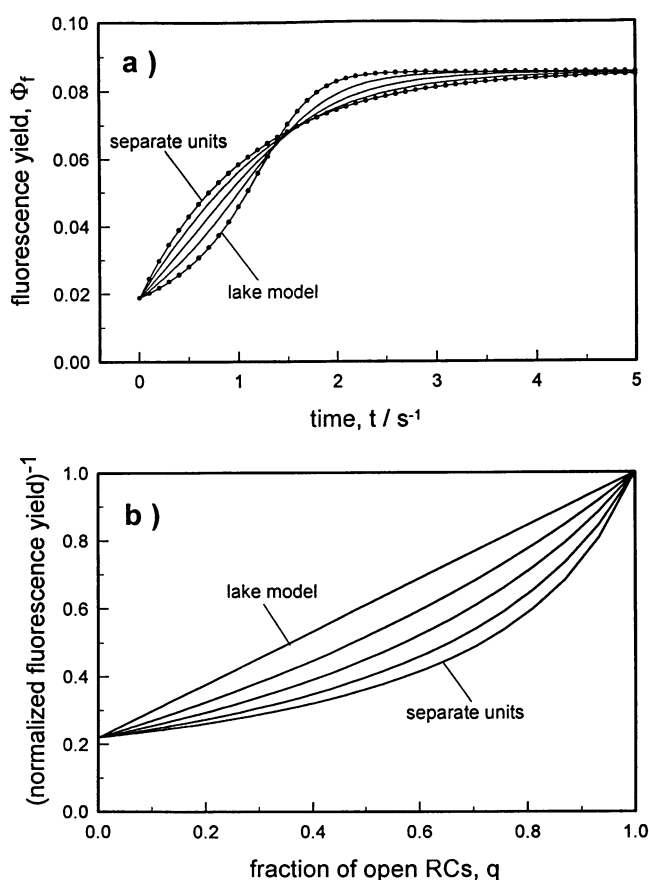
FIGURE 6  (a) Theoretical fluorescence induction curves calculated for different rate constants of interunit exciton transfer $k_{UU}$. The other rate constants were taken from Roelofs et al. (1992) for $\alpha$ centers: $k_t^{ox} = 3.00$ ns$^{-1}$, $k_{-1}^{ox} = 0.30$ ns$^{-1}$, $k_2 = 2.30$ ns$^{-1}$, $k_t^{red} = 0.47$ ns$^{-1}$, $k_{-1}^{red} = 0.34$ ns$^{-1}$, $k_d^{ox} = 0.00$ ns$^{-1}$, $k_d^{red} = 0.99$ ns$^{-1}$, $k_1 = 0.30$ ns$^{-1}$, Then, with $k_{rad} = 0.056$ ns$^{-1}$, one computes $\alpha_p = 2.653$ ns$^{-1}$, $\alpha_d = 0.0011$ ns$^{-1}$, $\beta = 0.350$ ns$^{-1}$, $J_{lake} = 3.54$, and $\Phi_m/\Phi_o = 4.54$. The intensity of excitation was $I = 1$ s$^{-1}$. ●, Plot of the results obtained for the lake model and isolated units by Trissl et al. (1993). b) Normalized Stern–Volmer plots of the same set of fluorescence induction curves. The $k_{UU}$ values (from isolated units to lake) are 0, 0.33, 1.00, 3.33, and $\infty$ ns$^{-1}$, and the $J$ values are 0, 0.36, 0.90, 1.88, and 3.54.

$$\Phi_f(q) = \frac{\Phi_m - q[\Phi_m - \Phi_o(1 + J)]}{1 + Jq},\tag{31}$$

and we obtain

$$\frac{\Phi_v(q)}{\Phi_v^m} = \frac{1 - q}{1 + Jq}.\tag{32}$$

This quotient is often called the photochemical quenching coefficient. Equation 32 is identical (we use $p$ instead of $J$; Eq. 9) to the equation derived under a much more restrictive set of assumptions by Joliot and Joliot (1964). The broader validity of this equation was pointed out before by Paillotin (1976b) and by Butler (1980) in the case of the tripartite model. This relation implies a linear dependence of $\Phi_v^m/(\Phi_v(q))$ on $1/(1 - q)$, with slope $(1 + J)$ and intercept $-J$. Such a double-reciprocal plot may be used for estimating the value of $J$ because $\Phi_v(q)$ can be obtained by integrating the induction curve (see below).

## Kinetic law

The integration procedure of Eqs. 10–12 remains fully valid in the most general case considered here, and so does the kinetic law, Eq. 12. As may be seen from Fig. 6 ($a$), the parameter $J$ is responsible for the degree of "sigmoidicity" of the fluorescence induction. The case $J = 0$ corresponds to an exponential kinetics reflecting the absence of exciton transfer from closed to open PS II units.

It is worth emphasizing that, in spite of the complications that were introduced in our general model (radical pair reversibility, consideration of two different pigment beds), the dependence of the normalized variable fluorescence on $q$ (Eq. 32) is controlled by one parameter ($J$), and its time course (Eqs. 12 and 32) is entirely determined by $J$ and by the time-scaling factor $I\Phi_p(1)$. Thus, in principle, these parameters are directly accessible from experimental kinetics, irrespectively of any particular model (complications that are due to PS II heterogeneity will be discussed below).

The yield expressions and the kinetic law keep the same form when one is considering an induction curve starting with a fraction of centers in the closed state (thus, with the initial fraction of open centers $q_0 < 1$). The apparent values of $\Phi_p(1)$ and $J$ are then

$$\Phi_p'(1) = \frac{1 + J}{1 + q_0 J}\Phi_p(1),\tag{33a}$$

$$J' = q_0 J.\tag{33b}$$

These relations are useful because the experimental curves obtained in the presence of DCMU frequently have an increased $F_o$ with respect to the level observed in the absence of an inhibitor. This reflects the reduction of $Q_A$ in centers where a semiquinone was present in the $Q_B$ pocket before the inhibitor was added. The effect of this prereduction of $Q_A$ on the induction may be estimated from Eqs. 33.

## Stern–Volmer relation

From Eq. 31, we get immediately

$$\frac{1}{\Phi_f(q)} = \frac{1 + Jq}{\Phi_m - q[\Phi_m - \Phi_o(1 + J)]}.\tag{34}$$

Thus, the Stern–Volmer relation (linearity of $\Phi_f(q)^{-1}$ versus $q$) is *not* obeyed in general, except in the special case when $\Phi_m = (1 + J)\Phi_o$ (this implies that $C = 0$ in Eq. 6a). For the connected units model the deviations from Stern–Volmer behavior are illustrated in Fig. 6 ($B$). The Stern–Volmer condition is fulfilled in the lake model (irrespective of the exciton–radical-pair equilibrium), as apparent from Eq. 5a. More generally, as may be seen from inspection of Eq. 28d, the condition $C = 0$ corresponds to two possibilities: i) the first is a trivial one (and obviously unacceptable on experimental grounds) where $k_{20} = k_{30}$, meaning equal trapping by open and closed RCs; ii) the second is that $C$ will also approach zero (while $A$ and $B$ remain finite) when any of the antenna transfer rate constants ($k_{AU}$, $k_{UA}$, $k_{UU}$) becomes very

large (barring the special case when both $k_{UU}$ and $k_{UA}$ are close to zero). Therefore, the deviation from the Stern–Volmer relation may be taken as an indicator of the degree of imperfect connectivity of units. As discussed below, $J$ also depends on the connectivity but, additionally, on properties of the RC.

## Complementarity of $\Phi_f$ versus $\Phi_p$

From Eq. 31 one obtains

$$\Phi_m - \Phi_f(q) = q\Phi_v^m \frac{1+J}{1+Jq}.\qquad(35)$$

Thus, when we use $\Phi_p(1) = A/(1 + J)$,

$$\Phi_p(q) = \Phi_p(1)\frac{\Phi_m - \Phi_f(q)}{\Phi_v^m},\qquad(36)$$

showing that for a homogeneous PS II domain the photochemical yield is linearly related to $(\Phi_m - \Phi_f)$. This relation does not hold, in general, when heterogenous contributions are present, except when the different components keep an identical value of the ratio $\Phi_v^m/\Phi_p(1) = (JB - C)/A$. As argued below, this condition is also necessary for a proportionality relation between the number of RCs and the area of the fluorescence induction (Eq. 41; see also Eq. 47). The experimental demonstration by Bennoun and Li (1973) of the complementary behavior of the photochemical and fluorescence yields during the induction kinetics suggests that the PS II$_\alpha$ and PS II$_\beta$ contributions meet this requirement, at least approximately.

## Complementary area of the fluorescence induction

Using Eq. 10 and expressing $\Phi_f$ as a function of time, it follows from Eq. 36 that

$$q(t) = 1 - \frac{I\Phi_p(1)}{\Phi_v^m}\int_0^t [\Phi_m - \Phi_f(\tau)]d\tau,\qquad(37)$$

which gives the familiar relation between the kinetics of $q$ and that of the complementary area of the fluorescence induction first derived by Malkin and Kok (1966) and Murata et al. (1966). This proportionality has also been reported in Trissl et al. (1993). We obtain the total area $\Phi_a$ that corresponds to a one-electron transfer per RC by taking $t \to \infty$:

$$\frac{I\Phi_p(1)}{\Phi_v^m}\Phi_a = 1.\qquad(38)$$

Again, these expressions are model independent and follow simply from the complementarity between the fluorescence and photochemical yields. Their validity does not depend on the degree of connectivity and is also verified in models involving domains containing a finite number of PSUs (Paillotin, 1976b; Den Hollander et al., 1983). However powerful, their practical applicability requires some care because of the factor multiplying the integral. To ana-

lyze this point further, we examine the relationship between the number of reaction centers and the experimental fluorescence area $F_a$ (obtained by integrating the kinetics of fluorescence *intensity* rather than the quantum yield). Let us assume a homogeneous array of PS II units with density [RC] (the number of centers per illuminated area unit). The fluorescence intensity is

$$F(q) = I[RC]\Phi_f(q).\qquad(39)$$

Thus

$$F_a = I[RC]\Phi_a,\qquad(40)$$

and, using Eqs. 38 and 6,

$$F_a = [RC]\frac{\Phi_v^m}{\Phi_p(1)} = \frac{JB - C}{A}[RC].\qquad(41)$$

Thus, $F_a$ is related to the number of centers through a factor depending on model parameters (e.g., rate constants). In the connected units model, this factor is

$$\frac{JB - C}{A} = k_{rad}\frac{\alpha_p + \alpha_d - \beta}{\alpha_p(\beta + k_1)}.\qquad(42)$$

On the one hand, the factor calculated in Eq. 42 does not depend on $k_{UU}$ and is thus insensitive to connectivity. On the other hand, it depends on the antenna size $N$ (number of light-harvesting pigments per RC) if the intrinsic trapping properties of the center are assumed to be fixed. Indeed, as we noted above, the effective rate constants for trapping an exciton from the whole antenna may be estimated as the ratio of intrinsic rate constants for the naked center, $k_t^{int}$, divided by $N$ ($k_t = k_t^{int}/N$). The same follows for $\alpha_p$, $\alpha_d$, and $\beta$. As already mentioned, the case of heterogeneous pigments can be accommodated by using an effective antenna size, $N_{eff}$. When expressed in terms of intrinsic parameters, the factor in Eq. 41 reads as

$$\frac{JB - C}{A} = k_{rad}\frac{\alpha_p^{int} + \alpha_d^{int} - \beta^{int}}{\alpha_p^{int}\left(\dfrac{\beta^{int}}{N} + k_1\right)}.\qquad(43)$$

This matter has an important bearing on the estimate of the relative amounts of $\alpha$ and $\beta$ centers from their contributions to the fluorescence area, as discussed below.

A case in which the estimate of the amount of centers from the fluorescence area is grossly in error is encountered when only a fraction of centers have a blocked $Q_B$ pocket and compete with uninhibited (permanently open) centers for exciton trapping. This situation occurs when one is studying the effect of a subsaturating concentration of DCMU and also, according to Lavergne and Leci (1993), in the absence of inhibitor when one is considering the $\Phi_o$–$\Phi_{pl}$ kinetics that are due to inactive PS II centers. Then, using Eqs. 14–15, and 18 from the appendix in Lavergne and Leci (1993), one gets

$$\frac{\Phi_a'}{\Phi_a} = \frac{\Phi_v^{m'}}{\Phi_v^m} = \frac{x}{1 + J(1 - x)},\qquad(44)$$

where the primed quantities correspond to the induction curve contributed by a fraction $x$ of inhibited centers in the presence of $1 - x$ permanent traps, whereas the unprimed quantities refer as usual to total inhibition. Thus, the relative area reflects only the relative variable fluorescence, and the computation of the amount of centers $x$ requires the knowledge of $J$.

## Genty's formula

Based on work of Kitajima and Butler (1975) and Schreiber et al. (1986), Genty et al. (1989) proposed an expression for estimating the photochemical yield of PS II during steady-state electron flow from fluorescence levels:

$$\Phi_p(q) = \frac{\Phi_m - \Phi_f(q)}{\Phi_m}, \tag{45}$$

which is different from our Eq. 38. In our notation Genty's formula is equivalent to

$$\nu_{O_2} = I[RC] \frac{\Phi_m - \Phi_f(q)}{\Phi_m}, \tag{46}$$

where $\nu_{O2}$ is the rate of electron transfer through PS II (as measured, e.g., from oxygen evolution, assuming the absence of a DCMU-type inhibitor; in the presence of such an inhibitor $-dq/dt$ may be used in place of $\nu_{O_2}$). Notice that Eqs. 45 and 46 may be written equally well in terms of $\Phi_f$ or $F$ because the $I[RC]$ factor is eliminated in the ratio. Equation 45 is quite convenient because it requires only two measurements: $F$ (e.g., a steady-state fluorescence level) and $F_m$ (obtained by photoreducing all $Q_A$ by a brief intense light pulse). It has been widely used for estimating the electron transfer rate in the presence of the nonphotochemical quenching that develops under steady-state illumination.

We would like to discuss the extent of its applicability. Combining Eqs. 6a and 6b, one gets

$$\frac{\Phi_m - \Phi_f(q)}{\Phi_m} = \frac{J B - C}{A B} \Phi_p(q). \tag{47}$$

For calculating the factor multiplying $\Phi_p$, we consider again the connected units model. Using Eqs. 42 and 30c, we obtain:

$$\frac{J B - C}{A B} = 1 + \frac{\alpha_d - \beta}{\alpha_p}. \tag{48}$$

This expression depends not on antenna parameters (size or connectivity) but only on intrinsic center parameters (the $1/N$ factors are eliminated when we write Eq. 48 in terms of intrinsic rate constants). Using the set of rate constants (see the caption to Fig. 6) of Roelofs et al. (1992) for PSII$_\alpha$, we obtain for Eq. 48 a value of 0.88, which suggests that omission of this correction may lead one to underestimate $\Phi_p$ by $\sim 14\%$.

Under steady-state illumination in vivo, both $\nu_{O_2}$ and $(F_m - F)/F_m$ decrease as a function of the intensity because of the nonphotochemical quenching $qN$. A linear relationship

has been observed between these quantities under a broad range of irradiance (with the exception of dim light), markedly modulating $qN$ (reviewed by Lavergne and Briantais, 1995). The present analysis suggests that this finding is not trivial and brings relevant information as to the origin of $qN$. First, the linear relationship is expected to hold if $qN$ is due to a quenching process in the antenna (as is believed to arise from aggregation of LHC II), which would increase $k_1$ and leave unchanged the proportionality factor (Eqs. 47 and 48). On the other hand, linearity should break down if $qN$ were due to the removal of a fraction of the PS II antenna (as in a state-2 transition; this phenomenon may in fact account for the dim-light deviation), because this would correspond to a decrease of $I$ in Eq. 46. A third possibility for $qN$ is that it involves a modification of the centers. If this modification is assumed to affect all centers in a homogeneous way, then the linearity should again break down (because an increase of $\alpha_d$ at the expense of $\alpha_p$ will increase the proportionality factor calculated in Eq. 48). In the case of an all-or-none process affecting a fraction of the centers, the outcome depends on the degree of connectivity. In a pure lake model, the conversion of a fraction of centers to quenching sinks will affect $\nu_{O_2}$ and $(F_m - F)/F_m$ in the same proportion. If, however, connectivity is finite, $\nu_{O_2}$ will be more diminished than $(F_m - F)/F_m$ when $qN$ develops. This is easily seen in the extreme case of isolated units. Let us assume that active units have fluorescence yields $\Phi$ (at steady state) and $\Phi_m$ (under a saturating pulse), while inactive units are blocked, say, at $\Phi_o$. If $f$ denotes the fraction of active units, the measured $F$ and $F_m$ will be

$$F = I[RC](\Phi f + \Phi_o(1 - f)), \tag{49a}$$

$$F_m = I[RC](\Phi_m f + \Phi_o(1 - f)), \tag{49b}$$

where $I[RC]$ indicates the rate of absorption in the whole system (active and inactive units). Then

$$\frac{F_m - F}{F_m} = \frac{f(\Phi_m - \Phi)}{\Phi_m} \frac{\Phi_m}{\Phi_m f + \Phi_o(1 - f)}, \tag{50}$$

whereas, under the above assumption, $\nu_{O_2}$ is just proportional to the first factor,

$$\frac{f(\Phi_m - \Phi)}{\Phi_m}.$$

## Significance of J

In the particular model analyzed by Joliot and Joliot (1964), a parameter $p$, related to our $J$ through Eq. 9, was defined as the probability that an exciton hitting a closed RC will be transmitted to an open RC. In the more general models described here, this definition does not hold rigorously, but a related physical meaning of $p$ or $J$ can nevertheless be given. If we define the effective cross section of an open center by

$$\sigma(q) = \frac{\Phi_p(q)}{q}, \tag{51}$$

where the photochemical yield $\Phi_p$ is given by Eq. 6b, we see

that

$$\frac{\sigma(0)}{\sigma(1)} = J + 1. \qquad (52)$$

Thus, $(J + 1)$ expresses the relative increase in cross section brought about by closing neighboring centers ($\sigma(1)$ is the minimum cross section and $\sigma(0)$ the maximum one). It may also be taken as an estimate of the effective number of units that an exciton can visit during its lifetime when $q = 0$.

The parameter $J$ depends on *both* antenna and center parameters. To analyze this in more detail, let us consider the expression found for $J$ in the connected units model (Eq. 30a). Using Eq. 7a, we can rewrite this expression as the product

$$J_{cu} = J_{lake} \frac{k_{UU}}{(k_{UU} + \alpha_p + \alpha_d + k_1)}, \qquad (53)$$

where the subscripts cu and lake refer to the connected units model and the lake model, respectively. Inspection of Eq. 7a shows that $J_{lake}$ is, as is intuitively clear, an increasing function of the trapping efficiency of the open center ($\alpha_p + \alpha_d$) and a decreasing function of the trapping efficiency of the closed center ($\beta$) and of losses in the antenna ($k_1$). Furthermore, $J_{lake}$ can be expressed by the extreme fluorescence levels (using Eqs. 7a, 8a, and 8c):

$$J_{lake} = \frac{\Phi_m}{\Phi_0} - 1. \qquad (54)$$

The decrease of $J$ brought about by the second factor in Eq. 53 is specific for imperfect connectivity of the antenna system. It makes $J$ an increasing function of the rate of interunit transfer $k_{UU}$ or, more precisely, a decreasing function of the ratio of the decay rate in open units ($\alpha_p + \alpha_d + k_1$) over $k_{UU}$.

Similar conclusions were attained in previous work by Paillotin (1976b) where it was pointed out that the connection parameter $p$ accounts for two separate processes: the actual exchange of excitons between units and the competition between centers for exciton capture. Paillotin derived the following equation for the connection parameter:

$$p = \omega\left(1 - \frac{\Phi_m}{\Phi_0}\right), \qquad (55)$$

in which $\omega$ is the probability of an exciton's leaving a PSU with a closed RC (toward another PSU). An equation of the same form is found in our formalism. Using Eqs. 7–9 and 30a (connected units model), one obtains

$$\omega = \frac{k_{UU}}{\beta + k_1 + k_{UU}}, \qquad (56)$$

which matches Paillotin's definition.

## APPLICATION TO EXPERIMENTAL DATA

### Validity of the foregoing treatment

*Extent of exciton migration in PS II*

Our basic assumption is to consider PS II an infinite array with an overall homogeneous character. We did consider

antenna heterogeneity (i.e., core and peripheral antennas) and finite connectivity, but we did not envisage domain heterogeneities, such as a finite size of domains for exciton migration including a small number of PS II centers (Clayton, 1967; Den Hollander et al., 1983). Thus, our modeling belongs to the "lake" family, although, for brevity, we have reserved the term "lake model" to unrestricted exciton diffusion in a homogeneous antenna (the "free exciton movement" case in the terminology of Paillotin, 1976b). In particular, our treatment does not apply to the case of a dimeric arrangement of PS II centers (Rögner et al., 1987; Dainese and Bassi, 1991; Peter and Thornber, 1991) insofar as one assumes that privileged excitation transfer occurs between the two partners of the dimer. Models of the domain type have been considered in earlier literature (Clayton, 1967; Paillotin, 1976a; Den Hollander et al., 1983). Expressions for the yields as a function of $q$ can be obtained in such models, too. The derivation of a kinetic equation for the fluorescence induction requires taking into account explicitly the evolution of the populations of domains with 0, 1, ...$n$ closed centers through a master equation (Den Hollander et al., 1983). In a previous report (Trissl and Lavergne, 1995), we examined the fitting of an experimental induction curve, using the equation derived by Den Hollander et al. (1983). An acceptable fit was obtained for a number of 4–5 centers per domain.

Obviously, it is expected that, when the number of centers per domain is increased beyond $(J + 1)$, such models will become indistinguishable from the infinite PS II case. Concerning the possibility that exciton transfer in PS II may be organized in domains with a small number (<4) of centers per domain, we believe that there is significant evidence against its plausibility, although it may not be completely ruled out. A first aspect is that fast spectroscopic techniques picture the PS II reaction center as a shallow trap that is visited by the exciton a number of times before stabilized trapping occurs (exciton–radical-pair equilibrium model, van Gorkom, 1985; Schatz et al., 1988; Leibl et al., 1989; Roelofs et al., 1992). This will tend to minimize the effect of the local arrangement of centers (for instance, in a dimeric structure). Furthermore, there is substantial evidence showing that exciton migration extends over many PSUs (Joliot et al., 1973; Paillotin, 1976a; Trissl et al., 1987; Garab, 1992). An important argument is the quasilinearity of the $\Phi_f$ versus $\tau_{av}$ (average fluorescence lifetime) observed during the induction, which would not hold for domains containing a small number of units (Sorokin, 1971; Briantais et al., 1972; Moya, 1974; Paillotin, 1976b; Lavorel and Etienne, 1977).

The interpretation of the sigmoidicity of the fluorescence induction (or the hyperbolic dependence of $\Phi_f$ on $q$) as reflecting excitonic connection of the RCs has been challenged (Ley and Mauzerall, 1986; France et al., 1992) on the grounds of an exponential saturation curve for charge separation induced by short (in the microsecond or submicrosecond range) light pulses (see, however, Hemelrijk and van Gorkom, 1992). We believe that this finding may be due to quenching processes on short time scales, such as exciton–exciton anihilation (Geacintov and Breton, 1987), quenching

by triplet states (Wolff and Witt, 1969, Breton et al., 1979; Geacintov and Breton, 1987), and P-680$^+$ (Butler, 1972, Sonneveld et al., 1979, Deprez et al., 1983). Even in the case of a "long" microsecond flash, a fluorescence rise (disappearance of a quenching) occurs in the 30–50-$\mu$s range (Joliot, 1974; Robinson and Crofts, 1987), possibly as a result of a slow phase of P-680$^+$ reduction (see also Schlodder et al., 1985). Such transient quenchings may severely affect the correlation between the excitation energy and the product yield (Deprez et al., 1990; Wulf and Trissl, 1994). In the pump–probe double-flash experiments of Geacintov et al. (1987) or France et al. (1992), 200–300-ps actinic flashes were used, and the fluorescence was analyzed 100 $\mu$s later by a weak microsecond flash. Clearly, no increase of the trapping cross section can be expected during the closure of centers by the 200-ps pulse, because closed centers remain in quenching state P-680$^+$ during the lifetime of the excitons. The cross section may, on the contrary, decrease at high flash energy as the result of singlet–singlet annihilation or quenching by triplet states. Thus, the course of the decrease of $q$ as a function of the flash energy cannot be faster than an exponential, but, presumably, is slower. Even in the conservative case of an exponential dependence, it should be realized that the fluorescence yield detected by the probe flash is expected to have a much less pronounced sigmoidicity as a function of the actinic energy than that observed during weak light induction. Assuming that $q(\epsilon) = e^{-\epsilon}$, where $\epsilon$ is proportional to the flash energy, one has from Eq. 32 $\Phi v(\epsilon)/\Phi vm = (1 - e - \epsilon)/(1 + Je - \epsilon)$. This function has no inflection point for $J < 1$, and, even for $J = 1.5$, the sigmoidal character may be hard to discern, depending on the experimental accuracy.

The fact that a hyperbolic dependence of the photochemical yield on the amount of open centers was established through oxygen-evolution measurements (Joliot et al., 1971), independently from (but in approximate agreement with) fluorescence data is a strong argument against models that reject excitonic connection as the major cause for the sigmoidal induction curves. The view of connected PS II is also supported by the finding of an increased antenna size in mutants that have a normal chlorophyll content but a smaller number of PS II centers (Joliot et al., 1973).

## Rapid exciton equilibration

In the mathematical formulation that we have used, the spatial location of the exciton is disregarded, allowing us to consider situations such as that of an exciton in antenna bed $A$ or $U$ as well-defined *states*. Similarly, the spatial distribution of open/closed centers is not taken into account. This considerable simplification could be questioned in the case of a strongly diffusion-limited trapping process. However, as argued above, PS II photochemistry is actually trap limited. In his recent review, Dau (1994) concludes that the available evidence supports the concept of rapid exciton equilibration among all pigments of the PS II antenna. Furthermore, it appears that, even considering a diffusion-limited process,

the inaccuracy involved in ignoring spatial coordinates of the excitons and centers is actually quite small. This emerges from comparison with the results of studies of exciton random walk that used the master equation approach (Paillotin, 1976a; Paillotin et al., 1983; Den Hollander et al., 1983) or the Monte Carlo method (Sebban and Barbet, 1985; Hoff and Fischer, 1993) or $N$ coupled differential equations controlled by a Pauli master equation (Laible et al., 1994). For instance, we verified that the relations deduced from our treatment simulate quite accurately the Monte Carlo results reported by Hoff and Fischer (1993) for the whole range of parameters (from trap to diffusion limitation) assayed by these authors.

## Radical pair reversibility

The implementation of the exciton–radical-pair equilibrium in the analysis of decay yields amounts to the introduction of modified rate constants (that we denoted $\alpha$ and $\beta$) in an equivalent irreversible scheme (Fig. 2; see also Dau, 1994). It should be realized that the description of the radical-pair dynamics in terms of rate constants may be an oversimplification because it neglects the evolution of the pair toward a manifold of substates. A first aspect that should be considered in that respect is spin dephasing. The pair $P^+I^-$ is initially created in its singlet state, but a singlet–triplet mixing process will then take place, and only the singlet state can recombine to an exciton. The dynamics of this process cannot be described by rate constants but requires a proper quantum-mechanical treatment (stochastic Liouville equation; see Haberkorn and Michel Beyerle, 1979, and the review by Hoff, 1981). It was, however, argued by van Gorkom (1985) that spin dephasing is probably slow with respect to the equilibrium with the exciton state (this fast equilibrium, together with the initial zero rate of the spin dephasing, could actually be responsible for delaying the process). A slow rate for singlet–triplet mixing was reported in the recent study by Volk et al. (1993) showing that, in the $D_1D_2cytb_{559}$ reaction center, spin dephasing occurs in the 100-ns time range (see also Groot et al., 1994). The light reemission from PS II is slightly enhanced by a magnetic field that decreases the yield of triplet formation (Rademaker et al., 1979), but most of the effect is probably due to an effect on delayed rather than prompt fluorescence (Hoff, 1981).

Whereas spin dephasing is probably a negligible perturbation in the exciton–radical-pair model, another type of evolution of the radical pair may have to be considered. Woodbury and Parson (1984) introduced the idea of a relaxation process in the free energy of the radical pair in the bacterial RC (and a similar view was proposed for PS II by Schlodder and Brettel, 1988). Further support for this concept was recently reported by Peloquin et al. (1994) and Woodbury et al. (1994), who proposed a "dynamic solvation model" in which the stabilization ($\Delta G$) of charge separation is rapidly increasing following initial radical-pair formation. If this model applies to PS II, then the use of rate constants for modeling the radical pair reversibility loses relevance. It is still possible, however, to use probabilities (the $p_{ij}$ as in Figs.

3 and 5; i.e. the overall probability for state $i$ to decay toward state $j$) that retain a clear physical sense.

## Analysis of an experimental induction curve

An experimental fluorescence induction curve from spinach thylakoids poisoned with DCMU is shown in Fig. 7 ($a$). In agreement with the concept of $\alpha/\beta$ heterogeneity (Melis and Homann, 1976, Melis and Duysens, 1979; for a recent review see Lavergne and Briantais, 1995), the data cannot be fitted
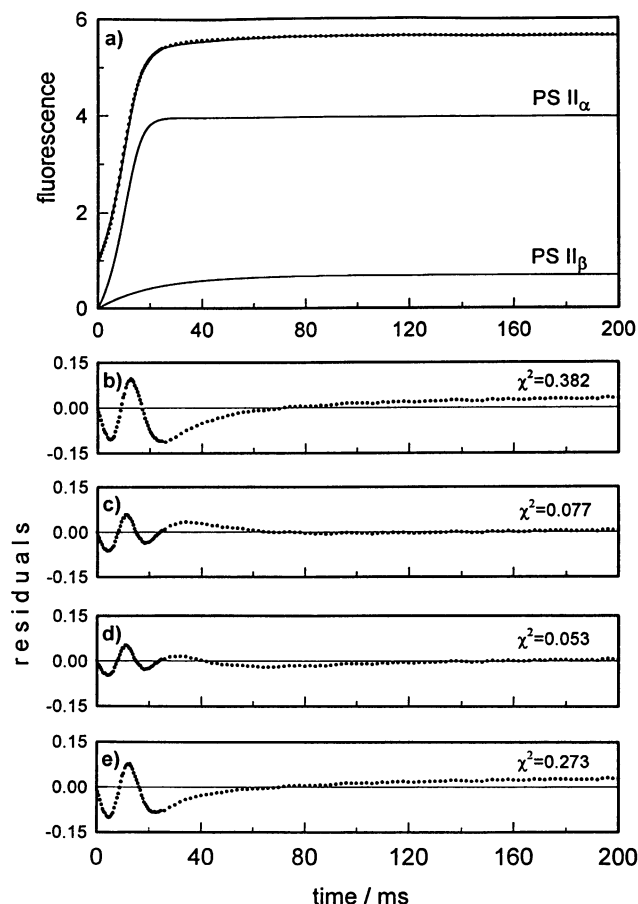


FIGURE 7  Experimental fluorescence induction curve and illustration of various fitting procedures. ($a$) ●, experimental datapoints, with normalization at $F_o = 1$. Spinach thylakoids at 10-mM Chl in a medium containing 0.3-M sucrose, 8-mM $MgCl_2$, 10-mM NaCl, and 25-mM MES, pH 6.5, with addition of 1-$\mu$M gramicidin and 20-$\mu$M DCMU. The cuvette was cylindrical, with an internal diameter of 3.2 mm. Actinic illumination was provided by symmetrically arranged arrays of light-emitting diodes (Hewlett Packard HLMA CL00, emission peak ~594 nm). Fluorescence was detected at 90° by a photodiode trough, a low-fluorescence Ulano Rubilith gelatin filter, and a long-path (30-mm) Schott RG-665 filter (a small correction was measured and applied for the residual offset that was due to stray light and filter fluorescence). The solid curve superimposed upon the data points is the result of the five-parameter fit also described in ($c$). The corresponding individual contributions of PS II$_\alpha$ and PS II$_\beta$ are also shown, with their vertical origin arbitrarily shifted at zero. ($b$)–($e$) Plots of residuals (experimental curve, $F^{exp}$ − calculated curve, $F^{cal}$) for the various fitting procedures described in the text. The values of $\chi^2 = \Sigma(F^{exp} - F^{cal})^2$ are indicated in each panel and may be used to rate the qualities of the fits. The values of the fitted parameters corresponding to ($b$)–($e$) are indicated in Table 2.

satisfactorily under the assumption of a single homogeneous system (see the larger residuals in Fig. 7 ($b$)). Much better fits (residuals in Fig. 7 ($c$) and ($d$)) can be obtained by assuming that, in addition to the main $\alpha$ component, a second ($\beta$) contribution is present, accounting for the slow "tail" of the induction curve.

According to the foregoing (Eqs. 12, 32, and 39), the contribution of any individual homogeneous PS II array to the variable fluorescence induction kinetics can be expressed analytically as a function of three phenomenological parameters: an amplitude parameter, $F_v^m$ ( $= I[RC]\Phi_v^m$), a rate parameter, $I\Phi_p(1)$, and the sigmoidicity parameter $J$. Within the general assumptions discussed in the preceding section, the functional dependence of the kinetics with respect to these parameters is the same, irrespective of detailed assumptions regarding antenna heterogeneity and connectivity, rate constants governing the exciton–radical-pair equilibrium, etc. If, however, the whole fluorescence curve (including the $F_o$) is taken into account, a fourth parameter is required that may or may not be constrained by the other ones, depending on the assumed model. For instance, if the extreme lake model is assumed, the sigmoidicity parameter $J$ is strictly related to the $F_m/F_o$ ratio (Eq. 54). Depending on the investigator's concern, the analysis of the fluorescence induction can be focused on the phenomenological parameters controlling the variable part (e.g., when the primary interest is a decomposition into $\alpha$ and $\beta$ components, without specifying detailed rate constants) or on a global analysis of the whole curve including the $F_o$, which means using Eq. 6a rather than Eq. 32 (e.g., when absolute yields or effects of rate constants are of interest). We have applied the first strategy in the fits corresponding to Fig. 7 ($b$)–($d$) and the second one in the case of Fig. 7 ($e$).

In the first approach, the decomposition of an experimental curve (variable part) into $\alpha$ and $\beta$ contributions can be obtained by running a nonlinear minimization procedure involving adjustment of six parameters (or five, if the $\alpha$ component is assumed exponential, i.e., with $J = 0$). We believe that this method of direct adjustment of the experimental curve is far more reliable than the usual procedure implying a semilog plot of the kinetics of the complementary area of fluorescence. The latter is extremely sensitive to the determination of the asymptotic level of fluorescence $F_m$, as pointed out by Bell and Hipkins (1985), and a further inaccuracy is involved in the determination of the amplitude and slope of the exponential component in the semilog plot. These problems are altogether avoided in the direct fit of the induction curve when analytical expressions are used for the $\alpha$ as well as for the $\beta$ component.

The fitting procedure used in Fig. 7 was Marquardt's algorithm according to Press et al. (1986). The $F_o$ level was first subtracted from the experimental induction curve, and the variable part was adjusted as a sum of two components (or only one in the case of Fig. 7 ($b$)). The routine requires the computation of the derivatives of the evaluation function with respect to each parameter: we obtained these analytically

with respect to $F_v^m$ and $I\Phi_p(1)$, (using Eqs. 32 and 12) and numerically with respect to $J$. We obtained the $q(t)$ function from the implicit Eq. 12, using a Newton–Raphson algorithm (Press et al., 1986). When it was taken into account, the $\beta$ component was assumed either exponential, involving two parameters (rate constant and amplitude) or sigmoidal (three parameters). Fig. 7 $(b)$–$(e)$ shows the residuals obtained in various cases, with parameters indicated in Table 2.

The residuals shown in Fig. 7 $(c)$ were obtained for the best fit of the experimental curve, assuming the traditional view of PS II$_\beta$ as an array of isolated units, with $J = 0$ (five-parameter fit). It may be compared with Fig. 7 $(b)$, where the absence of the $\beta$ contribution was assumed (three-parameters fit). The curve drawn in Fig. 7 $(a)$ is the kinetics computed in the five-parameter fit: as may be seen, the quality of the fit is quite satisfactory. A slight improvement was, however, obtained in the procedure used for Fig. 7 $(c)$ where the parameter $J$ of the $\beta$ contribution was freely adjustable (six-parameter fit), imposing no a priori assumption on the degree of connectivity of PS II$_\beta$. Similar parameters were obtained in the two latter cases for the $\alpha$ component. This component appears to have a large $J$ value in the particular experiment shown in Fig. 7 $(J \approx 2.45)$, which is thus at the top of the experimental range for this parameter. This may be compared with Fig. 4 of our previous paper (Trissl and Lavergne, 1995), where another experimental curve was analyzed, yielding a smaller $J$ ($\approx 1.5$) and also a larger $\beta$ component. The slightly improved fit obtained in the six-parameter adjustment (Fig. 7 $(d)$) compared with the classical model used in Fig. 7 $(c)$ shows that the experimental evidence allows the possibility of a certain degree of connectivity of PS II$_\beta$. It is clear, however, that the $J$ value for this component is, at any rate, much smaller than that of PS II$_\alpha$.

No significant change of the best-fit parameters was obtained when the five-parameter search procedure was run either on the 200-ms section of the induction shown in the figure, on a shorter section (down to 50 ms), or on the whole (1.3-s) experimental range. This suggests that if a third (slower) component were involved, its amplitude would have to be quite small. We do not exclude, however, that a treatment such as that designed by Hsu et al. (1989), using an adjustable asymptote with the goal of determining the slowest exponential contribution, might reveal the presence of such a component. The $\gamma$ phase described by these authors (Hsu and Lee, 1991) has an amplitude of less than 1% of $F_v^m$, and there is no evidence so far that it is related to a photoreduction of $Q_A$. The satisfactory stability of the parameter set obtained by our method when we vary the analyzed section shows its robustness and insensitivity to the experimenter's decision regarding the attainment of the asymptote.

The further use of the parameters thus derived, for estimating rate constants or the relative amount of the two types of PS II units, is model dependent. Nevertheless, one can directly obtain the complementary areas of each contribution from these parameters, using Eq. 38, as

$$F_a = \frac{F_v^m}{I\Phi_p(1)}. \tag{57}$$

As emphasized above, the relative concentration of the reaction centers belonging to each type of PS II is not in general simply proportional to the corresponding area, depending on the factor that appears in Eq. 41:

$$[RC] = \frac{F_v^m}{I\Phi_p(1)} \frac{A}{JB - C} = \frac{F_v^m}{I\Phi_p(1)} \frac{\alpha_p(\beta + k_1)}{k_{rad}(\alpha_p + \alpha_d - \beta)}, \tag{58}$$

where the latter expression, using Eq. 42, is restricted to the connected units model.

The two rightmost columns in Table 2 shows estimates of the interunit transfer rate $k_{UU}$. For the curves shown in Fig. 7 $(c)$ and $(d)$ the computation was based on the following assumptions. We assumed that the effective rate constants (rather than intrinsic rate constants for "naked centers") for exciton trapping were the same in PS II$_\alpha$ and PS II$_\beta$. This view

**TABLE 2 Fitted and computed parameters for the curves shown in Fig. 7**

| Panel in Fig. 7 | Fit Parameters | | | | | | Relative $\beta$ Area (%) | $k_{uu}^\alpha$ (ns$^{-1}$) | $k_{uu}^\beta$ (ns$^{-1}$) |
|---|---|---|---|---|---|---|---|---|---|
| | PS II$_\alpha$ | | | PS II$_\beta$ | | | | | |
| | $F_v^m$ | $I\Phi_p(1)$ | $J$ | $F_v^m$ | $I\Phi_p(1)$ | $J$ | | | |
| $(b)$ | 3.47 | 0.093 | 1.88 | – | – | – | – | 2.07 | – |
| $(c)$ | 2.97 | 0.099 | 2.51 | 0.51 | 0.046 | – | 27 | 3.59 | – |
| $(d)$ | 3.02 | 0.100 | 2.42 | 0.47 | 0.047 | 0.68 | 25 | 3.32 | 0.52 |
| $(e)$ | 3.21 | 0.095 | 2.14 | 0.26 | 0.065 | – | 10 | 1.8 | – |

In rows (b)–(d), the parameters corresponding to the best fit of the variable part of the experimental curve of Fig. 7 $(a)$ are indicated in the first columns. The fitting constraints were: no $\beta$ component in $(b)$ (three-parameter fit); exponential $\beta$ component in $(c)$ (five-parameter fit); sigmoidal $\beta$ component in $(d)$ (six-parameter fit). The relative $\beta$ area was computed according to Eq. 57. The interunit transfer rate $k_{UU}$ was computed from the following assumptions: connected units model with the same rate constants as indicated in the caption to Fig. 6, except $k_1 = 0.4$ ns$^{-1}$, $k_d^{red} = 0.50$ ns$^{-1}$, and $k_{-1}^{red} = 1.169$ ns$^{-1}$ (thus $\alpha_p = 2.654$ ns$^{-1}$, $\alpha_d = 0.0011$ ns$^{-1}$, and $\beta = 0.141$ ns$^{-1}$). As explained in the text, the modified rate constants were chosen to match the $F_m/F_o$ ratio of 5.65 obtained after subtracting the offset (25% of $F_o$) assumed for the PSI contribution. Row $(e)$ indicates the results of a different procedure, assuming the following constraints: the rate constants $\alpha_p$, $\alpha_d$, and $\beta$ are kept at the same values as above (for both PS II$_\beta$ and PS II$_\alpha$); the rate $(I)$ of photon absorption per PSU is the same in PS II$_\alpha$ and PS II$_\beta$ (same antenna size); the interunit transfer rate is negligible in PS II$_\beta$ ($J^\beta = 0$); the adjustable parameters are $k_1^\alpha$ (imposing $k_1^\alpha \geq 0.30$ ns$^{-1}$), $k_1^\beta$, and the relative amount of PS II$_\beta$. The best fit was obtained at the lower limit allowed for $k_1^\alpha$ (0.30 ns$^{-1}$), $k_1^\beta = 1.67$ ns$^{-1}$, a fraction of PS II$_\beta$ RCs of 32%, and other parameters as indicated in the table. The corresponding $\Phi_m/\Phi_o$ ratios were 6.66 and 2.39 for PS II$_\alpha$ and PS II$_\beta$, respectively.

is compatible with the rate constants (and their accuracy range) estimated by Roelofs et al. (1992) for both contributions, implying that the intrinsic rate constants must be significantly different (so that the effect of the smaller $N^\beta$ turns out to be roughly compensated). This implies that the two contributions have the same $\Phi_m/\Phi_o$ ratio and also that the relative amount of both photosystems can be directly obtained from the respective fluorescence areas (i.e., a fraction of $\beta$ PSUs near 25%). This also means that both components have the same photochemical yield, so that the ratio of the rate parameters $I\Phi_p(1)$ gives the ratio of the absorbed intensities or antenna sizes. Thus, under this assumption, a ratio of $N^\alpha/N^\beta \approx 2.1$ is obtained in the procedures shown in Fig. 7 (c) and (d).

The set of parameters estimated by Roelofs et al. (1992) implies that $\Phi_m/\Phi_o = 4.5$ (see the caption of Fig. 6). Although the raw $\Phi_m/\Phi_o$ of the curve in Fig. 7 (a) is close to this value, one should take into account the offset caused by the (fixed) fluorescence emission from PS I. As suggested by Trissl et al. (1993), the contribution of PS I to the fluorescence yield can be estimated to ~25% of $F_o$, from the known trapping time of $\tau_t \approx 90$ ps and the relation

$$\Phi_f^{PSI} = \frac{k_{rad}}{k_1 + k_t^{PSI}}, \tag{59}$$

provided that the spectral recording covers the main fluorescence emission bands (680 nm < $\lambda$ < 750 nm). Applying this correction to the curve of Fig. 7 (a), we get a value of $\Phi_m/\Phi_o = 5.6$ for the PS II contribution. To account for this constraint, we modified some of the rate constants in the following way. For the rate of antenna losses we adopted a value $k_1 = 0.4$ ns$^{-1}$, which is in the reported range for the fluorescence lifetime in LHC II. For $k_d^{red}$, we adopted a value of 0.5 ns$^{-1}$, as determined by Pokorny and Trissl (to be published). The value of $k_1^{red} = 1.169$ ns$^{-1}$ is then required to match the $\Phi_m/\Phi_o$ value, with all other rate constants kept at the values indicated in the caption of Fig. 6. The resulting estimates of $k_{UU}$ are indicated in Table 2, suggesting a value near 3 ns$^{-1}$ for PS II$_\alpha$).

If one had adopted the hypothesis that the intrinsic rate constants were identical for the "naked" $\alpha$ and $\beta$ RCs, different results would have been obtained for the relative antenna sizes and [RC] fractions of both contributions. The smaller $N^\beta$ would entail a larger photochemical yield $\Phi_p(1)$ for PS II$_\beta$, so that the ratio ($\approx 2.1$) of the $I\Phi_p(1)$ parameters of Table 2 (Fig. 7 (c) or (d)) would imply $N^\alpha/N^\beta = 2.3$. Similarly, using Eqs. 43 and 58 would yield a relative fraction of [RC]$^\beta$ of 32%, whereas the relative area (Fig. 7 (c)) is 27 %.

The residuals shown in Fig. 7 (e) illustrate an investigation of a specific model of PS II$_\beta$ based on the assumption that its lower photochemical efficiency is due not to a smaller antenna size but to increased quenching, caused, for instance, by neighboring PS I units. The simplest way to do this is to constrain all rate constants to keep identical values in PS II$_\alpha$ and PS II$_\beta$, except $k_1$ and $k_{UU}$. For simplicity, we assumed $k_{UU}^\beta = 0$, because it is clear (from comparison of Figs. 7 (c)

and (d)) that satisfactory fits imply a small $J$ for the $\beta$ contribution. The increased $k_1$ in PS II$_\beta$ is meant to mimick the additional quenching process, and a decreased $k_{UU}$ is expected from the dilution of PS II units within PS I units. The large $k_1^\beta$ needed to account for the slow rate of the $\alpha$ contribution entails a diminished $\Phi_m/\Phi_o$, which has to be compensated for by an increase in the $\Phi_m/\Phi_o$ of the $\alpha$ contribution. Under our set of rules, this means diminishing $k_1^\alpha$, and it turned out that the best fit under such conditions would require an unacceptably low value of this rate constant. We thus adopted $k_1^\alpha = 0.3$ ns$^{-1}$ as the lowest acceptable value. The resulting parameters are indicated in Table 2 and in its legend. This model (see Table 2) provides an additional illustration of a case in which the fraction of $\beta$ centers (32%) is different from their relative fluorescence area (10%). However, as may be seen from the residuals plot and the $\chi^2$ value in Fig. 7 (e), the resulting fit is far less satisfactory than those of Fig. 7 (c) and (d), which does not support a model of PS II$_\beta$ as "quenched PS II$_\alpha$."

The rather satisfactory fits of experimental induction kinetics by two-component models (Fig. 7 (c) and (d)) does not exclude that such models may represent an oversimplification. None of the residual plots shown in Fig. 7 (b)–(e) is random, and this may suggest that finer heterogeneities are involved. A greater number of discrete contributions may be envisaged that may arise for instance from granal, margin, and stromal regions (Albertsson et al., 1990) or from a continuous distribution of antenna sizes (Joliot et al., 1973). A related effect may be expected from the unavoidable light gradient resulting from the absorption of light by the top membrane layers with respect to the illumination beam (Leibl and Trissl, 1990; Paillotin et al., 1993; Meszéna and Westerhoff, 1994). Although a detailed discussion of these possibilities is beyond the scope of the present paper, a few remarks can be made. A continuous distribution of antenna sizes or a light-gradient effect should blur the sigmoidicity of the observed curve with respect to that of the individual components. Thus, the apparent $J$ would be decreased. This may affect the discussion given below, inferring a limited rate of interunit transfer from the comparison of $J$ with the $\Phi_m/\Phi_o$ ratio.

An important clue for analyzing such problems is the "reprise effect" described by Joliot et al. (1973) (see also Lavorel and Etienne, 1977). After a first complete induction curve from dark-adapted material is monitored, a second illumination is given before the recombination of closed RCs is completed. The second curve thus obtained is not superimposable upon the corresponding final portion of the dark-adapted one but is markedly faster. The interpretation given by Joliot et al. (1973) is a heterogeneity of antenna sizes. The final portion of the dark-adapted induction is dominated by contributions from "slow" domains with smaller antenna sizes. If the recombination process does not depend on the antenna size, this selection will be absent in the initial state of the second experiment, accounting for faster kinetics. Although this effect is expected to be due predominantly to the $\alpha/\beta$ heterogeneity, especially if the recombination of PS II$_\beta$

is slower than that of PS $II_\alpha$ (Melis and Homann, 1976; Thielen and van Gorkom, 1981), some data suggest that it is also present in the individual $\alpha$ contribution (Thielen and van Gorkom, 1981). Further investigation of this problem is needed before a definite conclusion is reached on the degree of heterogeneity of the $\alpha$ contribution.

## Lake model versus finite connectivity

The numerical estimates shown in Table 2 suggest that the interunit transfer rate $k_{UU}$ is not infinitely large but has a value in the same range as the trapping rate constant ($k_t^{ox}$ or $\alpha_p$). Fig. 8 shows a plot of the theoretical dependence of $J$ on $k_{UU}$ in the connected units model, adopting for all other rate constants the Roelofs set (caption of Fig. 6). As may be seen, the experimental range of $J$ (1–2.5) implies a range of 1–6 ns$^{-1}$ for $k_{UU}$ and thus suggests that the organization of PS $II_\alpha$ lies midway between the lake and isolated units cases.

This conclusion can be attained on a more general basis, i.e. without adopting a detailed set of rate constants values. Experimental induction curves provide two basic constraints that should be accommodated by theoretical modeling. The ratio $F_m/F_o$ is typically 4 (range of 3–5). On the other hand, the sigmoidicity corresponds to $J$ in the 1–2.5 range (typically 1.5). It is obvious that these constraints are not consistent with the simple lake model of unrestricted exciton diffusion, because for this case Eq. 54 predicts a much too small typical value of $\Phi_m/\Phi_o = 2.5$ for $J = 1.5$. The contradiction is especially significant if one takes into account the offset caused by PS I fluorescence (which we estimate to ~25% of the $F_o$) to the measured fluorescence levels. The $\Phi_m/\Phi_o$ ratio of PS II computed by subtracting this offset is significantly larger than the apparent $\Phi_m/\Phi_o$. If we take the values estimated for the experimental curve of Fig. 7 ($a$), $J_{lake}$ ($=\Phi_m/\Phi_o - 1$) is 4.6, whereas the fitted $J$ value is ~2.5. Equation 54 is also the condition for the applicability of the Stern-Volmer relation (see Eq. 34). As documented in Fig. 9, a marked deviation from the Stern–Volmer behavior is
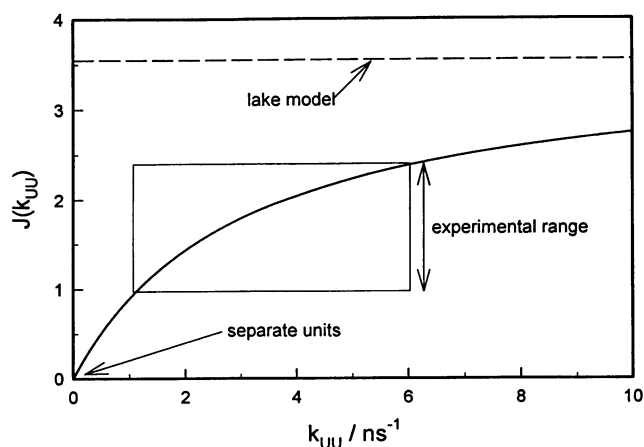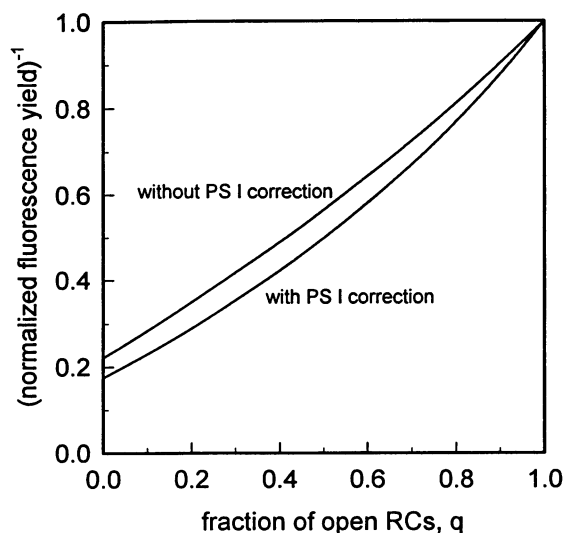
FIGURE 9   Normalized Stern–Volmer plots for $\alpha$ centers resulting from the best fit to the data of Fig. 7 ($a$) under the assumption of $\beta$ centers' being isolated units (five-parameters fit of Fig. 7 ($c$)). Effect of subtracting a constant fluorescence level (25% of the experimental $F_o$) as a result of PS I before data analysis.

observed for the $\alpha$ contribution in the kinetics of Fig. 7 ($a$), consistent with significant limitation of the interunit transfer.

In his study of the dependence of the average fluorescence lifetime $\tau_{av}$ on $\Phi_f$, Moya (1974) had similarly concluded in favor of a connected units model, with a value of $k_{UU}$ in the range 1 ns$^{-1}$ to 1.7 ns$^{-1}$. This was inferred from the slight negative concavity of this relationship, whereas the pure lake model would predict a linear dependence. Moya noticed that this curvature could not be ascribed to the offset that is due to PS I fluorescence, which would actually cause an opposite concavity (and may thus minimize the experimental curvature). Using equations derived for the tripartite model that corresponds to the funneling model described above, Butler (1980) also reported that experimental data were in better agreement with PS II being organized as a connected package rather than a matrix (i.e., lake).

## Connectivity in other photosystems

### Photosystem I

No variable fluorescence from PS I occurs under routine (i.e., oxidizing) experimental conditions because the reduced primary acceptor does not accumulate and the accessible closed state of the center, P-700$^+$, is an efficient quencher. In the presence of dithionite, however, the reduced acceptor can be photoaccumulated, and a fluorescence rise is observed (Ikegami, 1976). The connectivity of PS I units was investigated under such conditions in algae by Delepelaire and Bennoun (1978), who observed a twofold enlargement of the cross section of the remaining open centers when 80% of the centers were closed. The value of $J$ in PS I is thus close to 1. The available data do not allow a choice between the lake model or a more restricted connectivity.

FIGURE 8   Dependence of the sigmoidicity parameter $J$ on the rate constant of interunit exciton transfer, $k_{UU}$. Rate constants as in Fig. 6.

*Purple bacteria*

In contrast with PS I or PS II, the $P^+$ state of the reaction center of purple bacteria is not an efficient quencher and, in fact, the $F_m/F_o$ ratio is larger when centers are closed in the $P^+Q_A$ state than in the $PQ_A^-$ state (3.3 and 2.0, respectively in *R. rubrum*, according to Kingma et al., 1983). The Stern–Volmer behavior (linearity of $(\Phi_v^m)^{-1}$ versus the amount of open centers) has been demonstrated in this strain by Vredenberg and Duysens (1963) when the centers become closed by accumulation of the $P^+Q_A$ state. This result was confirmed and extended to the $PQ_A^-$ state by Kingma et al. (1983). Therefore, the lake model applies to a good approximation in this material, with $J$ near 1 or 2.3 on accumulation of, respectively, $PQ_A^-$ or $P^+Q_A$.

The picture that emerges from recent investigations (Timpmann et al., 1993, Otte et al., 1993, Beekman et al., 1994, Xiao et al., 1994) of the decay lifetimes or fluorescence action spectra in various purple bacteria is clearly different from the case of PS II with respect to radical pair reversibility. In these bacteria, the transfer from the antenna to the open RC appears to be the rate-limiting step in the trapping process, and the probability for backtransfer of the excitation from the trap to the antenna has been found in the range of 5–30%. To account for the data of Duysens and co-workers showing efficient energy transfer from closed to open centers, a larger escape probability must occur when centers are closed in the $PQ_A^-$ state. If one assumes rapid exciton equilibration in the antenna and a rate-limiting step between antenna and RC (similarly to the bipartite model of Butler and Kitajima, 1975), the problem can be handled in the present framework, using the funneling model, with $A$ standing for the antenna and $U$ for the RC. One can then obtain the constraints imposed on the rate constants to account simultaneously for the Stern–Volmer behavior (i.e., $|C/B| \ll 1$; Eq. 6a) and the experimental values of $\Phi_p(1)$ and $F_m/F_o$. The relative escape probabilities from the open/closed center can also be directly obtained if one adopts the lake model (Fig. 3) as a starting point (in agreement with Duysens' findings). Then, using Eqs. 15 and 18, one has

$$F_o \propto \frac{p_{10}}{1 - p_{12}p_{21}}, \tag{60a}$$

$$F_m \propto \frac{p_{10}}{1 - p_{13}p_{31}}, \tag{60b}$$

where the escape probabilities are $p_{21}$ and $p_{31}$ from, respectively, the open and closed centers. Assuming that $p_{12} \approx 1$ (imposed by the high photochemical yield) and $p_{12} \approx p_{13}$, one gets

$$\frac{F_m}{F_o} \approx \frac{1 - p_{21}}{1 - p_{31}}. \tag{61}$$

The escape probabilities in *R. rubrum* have been experimentally estimated by Timpmann et al. (1993), who found that $p_{21} = 25 \pm 5\%$ and $p_{31} = 40 \pm 5\%$ and thus an upper estimate of 1.45 for the right-hand part of Eq. 61, to be compared with the $F_m/F_o$ ratio of 2.

## CONCLUSION

The main purpose of this work was to derive explicit formulas for the analysis of fluorescence induction curves in a theoretical framework including exciton–radical-pair equilibrium and the possibility of modulating the efficiency of exciton transfer between PS II units. We have shown that these features do not preclude the outcome of simple general expressions and, in particular, do not affect the kinetic law derived in a more restrictive model by Joliot and Joliot (1964). The exciton–radical-pair equilibrium model is properly taken into account by adapting the values of the rate constants in an equivalent scheme with irreversible decay. The parameter $J$, controlling the sigmoidicity of the fluorescence induction, depends on both the decay pathway on the closed center and the efficiency of interunit transfer ($k_{UU}$). Interestingly, the latter parameter specifically affects the relation between $J$ and $\Phi_m/\Phi_o$ and, in a related way, the degree of curvature in the Stern-Volmer plot ($1/\Phi_f$ versus $q$). The analysis of experimental results along these lines supports the view of a limited interunit transfer (finite $k_{UU}$) rather than the pure lake model with free-exciton motion. We believe that the functional antenna organization of PS II represents an intermediate case well discernable from the extremes, namely, the lake and the separate unit models.

In the comment paper accompanying the paper by Trissl et al. (1993), Holzwarth (1993) asked the provocative question: "Is it time to throw away your apparatus for chlorophyll fluorescence induction?" This was motivated by the somewhat detructive picture emerging from the paper by Trissl et al. We hope that the present results will prompt a negative answer to Holzwarth's question. The analytical formulas that we have established allow a clarification of the conclusions attained in the paper by Trissl et al. (1993) from results obtained by numerical integration. One of these conclusions, rejecting the validity of Eq. 38, was merely an error. Others remain valid, such as the fact that broadly used relations between fluorescence area and the amount of centers, or between fluorescence levels and the photochemical yield, are not independent of the assumed set of rate constants for exciton migration and decay. This does not mean, however, that these relations are meaningless or useless, provided that the nature of their "model dependence" is clearly realized.

## REFERENCES

Albertsson, P.-Å., E. Andreasson, and P. Svensson. 1990. The domain organization of the plant thylakoid membranes. *FEBS Lett.* 273:36–40.

Beekman, L. M. P., F. van Mourik, M. R. Jones, H. M. Visser, C. N. Hunter,

and R. van Grondelle. 1994. Trapping kinetics in mutants of the photosynthetic purple bacterium *Rhodobacter sphaeroides:* influence of the charge separation rate and consequences for the rate-limiting step in the light-harvesting process. *Biochemistry.* 33:3143–3147.

Bell, D. H., and M. F. Hipkins. 1985. Analysis of fluorescence induction curves from pea chloroplasts. Photosystem II reaction centre heterogeneity. *Biochim. Biophys. Acta.* 807:255–262.

Bennoun, P., and Y.-S. Li. 1973. New results on the mode of action of 3,-(3,4-dichloro-phenyl)-1,1-dimethyl-urea in spinach chloroplasts. *Biochim. Biophys. Acta.* 292:162–168.

Breton, J., N. E. Geacintov, and C. E. Swenberg. 1979. Quenching of fluorescence by triplet excited states in chloroplasts. *Biochim. Biophys. Acta.* 548:616–635.

Briantais, J.-M., H. Merkelo, and Govindjee. 1972. Lifetime of the excited state *in vivo*. III. Chlorophyll during fluorescence induction in *Chlorella pyrenoidosa. Photosynthetica.* 6:133–141.

Butler, W. L. 1972. On the primary nature of fluorescence yield changes associated with photosynthesis. *Proc. Natl. Acad. Sci. USA.* 69:3420–3422.

Butler, W. L. 1978. Energy distribution in the photochemical apparatus of photosynthesis. *Annu. Rev. Plant Physiol.* 29:345–378.

Butler, W. L. 1980. Energy transfer between photosystem II units in a connected package model of the photochemical apparatus of photosynthesis. *Proc. Natl. Acad. Sci. USA.* 77:4697–4701.

Butler, W. L., and M. Kitajima. 1975. Fluorescence quenching in photosystem II of chloroplasts. *Biochim. Biophys. Acta.* 376:116–125.

Clayton, R. K. 1967. An analysis of the relations between fluorescence and photochemistry during photosynthesis. *J. Theor. Biol.* 14:173–186.

Dainese, P., and R. Bassi. 1991. Subunit stoichiometry of the chloroplast photosystem II antenna system and aggregation state of the component chlorophyll-*a/b* binding proteins. *J. Biol. Chem.* 266:8136–8142.

Dau, H. 1994. Molecular mechanisms and quantitative models of variable photosystem II fluorescence. *Photochem. Photobiol.* 60:1–23.

Delepelaire P., and P. Bennoun. 1978. Energy transfer and site of energy trapping in photosystem I. *Biochim. Biophys. Acta.* 502:183–187.

Den Hollander, W. T. F., J. G. C. Bakker, and R. van Grondelle. 1983. Trapping, loss and annihilation of excitations in a photosynthetic system. I. Theoretical aspects. *Biochim. Biophys. Acta.* 725:492–507.

Deprez, J., A. Dobek, N. E. Geacintov, G. Paillotin, and J. Breton. 1983. Probing fluorescence induction in chloroplasts on a nanosecond time scale utilizing picosecond laser pulse pairs. *Biochim. Biophys. Acta.* 725:444–454.

Deprez, J., G. Paillotin, A. Dobek, W. Leibl, H.-W. Trissl, and J. Breton. 1990. Competition between energy trapping and exciton annihilation in the lake model of the photosynthetic membrane of purple bacteria. *Biochim. Biophys. Acta.* 1015:295–303.

Duysens, L. N. M. 1979. Transfer and trapping of excitation energy in photosystem II. *In* Chlorophyll Organization and Energy Transfer in Photosynthesis. G. Wolstenholme and D. W. Fitzsimons, editors. CIBA Found. Symp. 61 (new series). Excerpta Medica, Amsterdam, New York. 323–340.

Duysens, L. N. M., and H. E. Sweers. 1963. Microalgae and Photosynthetic Bacteria. Japanese Society of Plant Physiologists, editor. University of Tokyo Press, Tokyo. 353–372.

Falkowski, P. G., Z. Kolber, and D. Mauzerall. 1994. A comment on the call to throw away your fluorescence induction apparatus. *Biophys. J.* 66:923–928.

France, L. L., N. E. Geacintov, J. Breton, and L. Valkunas. 1992. The dependence of the degrees of sigmoidicities of fluorescence induction curves in spinach chloroplasts on the duration of actinic pulses in pump-probe experiments. *Biochim. Biophys. Acta.* 1101:105–119.

Garab, G. 1992. Macrodomain organization of complexes in the thylakoid membranes. *In* Research on Photosynthesis. Vol. I. N. Murata, editor. Kluwer Academic Publishers, Dordrecht. 171–178.

Geacintov, N. E., J. Breton, L. France, J. Deprez, and A. Dobek. 1987. Laser flash-induced non-sigmoidal fluorescence induction curves in chloroplasts. *In* Progress in Photosynthesis Research, Vol. 1. J. Biggins, editor. Martinus Nijhoff Publishers, Dordrecht. 107–110.

Geacintov, N. E., and J. Breton. 1987. Energy transfer and fluorescence mechanisms in photosynthetic membranes. *Crit. Rev. Plant Sci.* 5:1–44.

Genty, B., J.-M. Briantais, and N. R. Baker. 1989. The relationship between

the quantum yield of photosynthetic electron transport and quenching of chlorophyll fluorescence. *Biochim. Biophys. Acta.* 990:87–92.

Govindjee and P. A. Jursinic. 1979. Photosynthesis and fast changes in light emission by green plants. *In* Photochem. Photobiol. Rev., Vol. 4. K. C. Smith, editor. Plenum Press, New York. 125–205.

Groot, M.-L., E. J. G. Peterman, P. J. M. van Kan, I. H. M. van Stokkum, J. P. Dekker, and R. van Grondelle. 1994. Temperature-dependent triplet and fluorescence quantum yields of the photosystem II reaction center described in a thermodynamic model. *Biophys. J.* 67:318–330.

Haberkorn, R., and M. E. Michel Beyerle. 1979. On the mechanism of magnetic fields effects in bacterial photosynthesis. *Biophys. J.* 26:489–498.

Hemelrijk, P. W., and H. J. van Gorkom. 1992. No double hit involved in fluorescence induction of photosystem II of spinach chloroplasts. *In* Research in Photosynthesis. Vol. II. N. Murata, editor. Kluwer Academic Publishers, Dordrecht. 33–36.

Hoff, A. J. 1981. Magnetic field effects on photosynthetic reactions. *Q. Rev. Biophys.* 14:4, 599–665.

Hoff, A. J., and M. R. Fischer. 1993. Excitation migration and trapping in homogeneous and heterogeneous lattices. Application to the light-harvesting antenna complex of photosynthetic bacteria. *Mol. Phys.* 78:799–819.

Holzwarth, A. R. 1993. Is it time to throw away your apparatus for chlorophyll fluorescence induction? *Biophys. J.* 64:1280–1281.

Hsu, B.-D., and J.-Y. Lee. 1991. A study on the fluorescence induction curve of the DCMU-poisoned chloroplast. *Biochim. Biophys. Acta.* 1056:285–292.

Hsu, B.-D., Y.-S. Lee, and Y.-R. Jang. 1989. A method for analysis of fluorescence induction curve from DCMU-poisoned chloroplasts. *Biochim. Biophys. Acta.* 975:44–49.

Ikegami, I. 1976. Fluorescence changes related in the primary photochemical reaction in the P-700-enriched particles isolated from spinach chloroplasts. *Biochim. Biophys. Acta.* 449:245–258.

Joliot, A. 1974. Fluorescence rise from 36 ms on following a flash at low temperature ($+2°$—$60°$). *In* Proceedings of the Third International Congress on Photosynthesis. Vol. 2. M. Avron, editor. Elsevier Scientific Publishing Company, Amsterdam. 315–322.

Joliot, P., A. Joliot, and B. Kok. 1968. Analysis of the interactions between the two photosystems in isolated chloroplasts. *Biochim. Biophys. Acta.* 153:635–652.

Joliot, P., A. Joliot, B. Bouges, and G. Barbieri. 1971. Studies of system II photocenters by comparative measurements of luminescence, fluorescence, and oxygen emission. *Photochem. Photobiol.* 14:287–305.

Joliot, P., P. Bennoun, and A. Joliot. 1973. New evidence supporting energy transfer between photosynthetic units. *Biochim. Biophys. Acta.* 305:317–328.

Joliot, P., and A. Joliot. 1964. Études cinétique de la réaction photochimique libérant l'oxygene au cours de la photosynthese. *C. R. Acad. Sci. Paris.* 258:4622–4625.

Kingma, H., L. N. M. Duysens, and R. van Grondelle. 1983. Magnetic field-stimulated luminescence and a matrix model for energy transfer. A new method for determining the redox state of the first quinone acceptor in the reaction center of whole cells of *Rhodospirillum rubrum. Biochim. Biophys. Acta.* 725:434–443.

Kitajima, M., and W. L. Butler. 1975. Quenching of chlorophyll fluorescence and primary photochemistry in chloroplasts by dibromothymoquinone. *Biochim. Biophys. Acta.* 376:105–115.

Laible, P. D., W. Zipfel, and T. G. Owens. 1994. Excited state dynamics in chlorophyll-based antennae: the role of transfer equilibrium. *Biophys. J.* 66:844–860.

Lavergne, J., and J.-M. Briantais. 1995. Photosystem II heterogeneity. *In* Oxygenic Photosynthesis: The Light Reactions. D. R. Ort and C. F. Yocum, editors. Series Advances in Photosynthesis. Kluwer Academic Publishers, Dordrecht. (in press).

Lavergne, J., and E. Leci. 1993. Properties of inactive photosystem II centers. *Photosynth. Res.* 35:323–343.

Lavorel, J., J. Breton, and M. Lutz. 1986. Methodological principles of measurements of light emitted by photosynthetic systems. *In* Light emission by plants and bacteria. Govindjee, J. Amesz, and D. C. Fork, editors. Academic Press, Orlando. 57–98.

Lavorel, J., and A.-L. Etienne. 1977. In vivo chlorophyll fluorescence. *In*

Topics in Photosynthesis. Vol. 2. Primary Processes of Photosynthesis. J. Barber, editor. Elsevier/North-Holland Biomedical Press, Amsterdam. 203–268.

Leibl, W., J. Breton, J. Deprez, and H.-W. Trissl. 1989. Photoelectric study on the kinetics of trapping and charge stabilization in oriented PS II membranes. *Photosynth. Res.* 22:257–275.

Leibl, W., and H.-W. Trissl. 1990. Relationship between the fraction of closed photosynthetic reaction centers and the amplitude of the photovoltage from light-gradient experiments. *Biochim. Biophys. Acta.* 1015: 304–312.

Ley, A. C., and D. Mauzerall. 1986. The extent of energy transfer among photosystem II reaction centers in *Chlorella*. *Biochim. Biophys. Acta.* 850:234–248.

Malkin, S., and B. Kok. 1966. Fluorescence induction studies in isolated chloroplasts. I. Number of components involved in the reaction and quantum yields. *Biochim. Biophys. Acta.* 126:413–432.

Melis, A., and L. N. M. Duysens. 1979. Biphasic energy conversion kinetics and absorbance difference spectra of photosystem II of chloroplasts. Evidence for two different photosystem II reaction centers. *Photochem. Photobiol.* 29:373–382.

Melis, A., and P. H. Homann. 1976. Heterogeneity of the photochemical centers in system II of chloroplasts. *Photochem. Photobiol.* 23:343–350.

Meszéna, G., and H. V. Westerhoff. 1994. Light intensity distribution in thylakoids and the polarity of the photovoltaic effect. *Biophys. Chem.* 48:321–336.

Moya, I. 1974. Duree de vie et rendement de fluorescence de la chlorophylle in vivo. Leur relation dans differents modeles d'unites photosynthetiques. *Biochim. Biophys. Acta.* 368:214–227.

Murata, N., M. Nishimura, and A. Takamiya. 1966. Fluorescence of chlorophyll in photosynthetic systems. II. Induction of fluorescence in isolated spinach chloroplasts. *Biochim. Biophys. Acta.* 120:23–33.

Otte, S. C. M., F. A. M. Kleinherenbrink, and J. Amesz. 1993. Energy transfer between the reaction center and the antenna in purple bacteria. *Biochim. Biophys. Acta.* 1143:84–90.

Paillotin, G. 1976a. Capture frequency of excitations and energy transfer between photosynthetic units in the photosystem II. *J. Theor. Biol.* 58: 219–235.

Paillotin, G. 1976b. Movement of excitations in the photosynthetic domains of photosystem II. *J. Theor. Biol.* 58:237–252.

Paillotin, G., N. E. Geacintov, and J. Breton. 1983. A master equation theory of fluorescence induction, photochemical yield, and singlet-triplet exciton quenching in photosynthetic systems. *Biophys. J.* 44:65–77.

Paillotin, G., A. Dobek, J. Breton, W. Leibl, and H.-W. Trissl. 1993. Why does the light-gradient photovoltage from photosynthetic organelles show a wavelength-dependent polarity? *Biophys. J.* 65:979–985.

Peloquin, J. M., J. A. C. Williams, X. Lin, R. G. Alden, A. K. W. Taguchi, J. P. Allen, and N. W. Woodbury. 1994. Time-dependent thermodynamics during early electron transfer in reaction centers from *Rhodobacter sphaeroides*. *Biochemistry.* 33:8089–8100.

Peter, G. F., and J. P. Thornber. 1991. Biochemical evidence that the higher plant photosystem II core complex is organized as a dimer. *Plant Cell Physiol.* 32:1237–1250.

Press, W. H., B. P. Flannery, S. A. Teukolsky, and W. T. Vetterling. 1986. Numerical Recipes. Cambridge University Press, Cambridge.

Rademaker, H., A. J. Hoff, and L. N. M. Duysens. 1979. Magnetic field-induced increase of the yield of (bacterio) chlorophyll emission of some photosynthetic bacteria and of *Chlorella vulgaris*. *Biochim. Biophys. Acta.* 546:248–255.

Robinson, G. W. 1967. Excitation transfer and trapping in photosynthesis. *In* Energy conversion by the photosynthetic apparatus. Brookhaven Symposia in Biology, Number 19. Brookhaven National Laboratory, Upton, New York. 16–48.

Robinson, H., and A. Crofts. 1987. Kinetics of the changes in oxidation-reduction states of the acceptors and donors of photosyszem II in pea thylakoids measured by flash fluorescence. *In* Progress in Photosynthesis Research. Vol. II. J. Biggins, editor. Martinus Nijhoff Publishers, Dordrecht. 429–432.

Roelofs, T. A., C.-H. Lee, and A. R. Holzwarth. 1992. Global target analysis of picosecond chlorophyll fluorescence kinetics from pea chloroplasts. A new approach to the characterization of the primary processes in photosystem II a- and b-units. *Biophys. J.* 61:1147–1163.

Rögner, M., J. P. Dekker, E. J. Boekema, and H. T. Witt. 1987. Size, shape and mass of the oxygen-evolving photosystem II complex from the thermophilic cyanobacterium *Synechocuccus* sp. *FEBS Lett.* 219:207–211.

Schatz, G. H., H. Brock, and A. R. Holzwarth. 1988. Kinetic and energetic model for the primary processes in photosystem II. *Biophys. J.* 54: 397–405.

Schlodder, E., and K. Brettel. 1988. Primary charge separation in closed photosystem II with a lifetime of 11 ns. Flash-absorption spectroscopy with O$_2$-evolving photosystem II complexes from *Synechococcus*. *Biochim. Biophys. Acta.* 933:22–34.

Schlodder, E., K. Brettel, and H. T. Witt. 1985. Relation between microsecond reduction kinetics of photooxidized chlorophyll $\alpha_{II}$ (P-680) and photosynthetic water oxidation. *Biochim. Biophys. Acta.* 808:123–131.

Schreiber, U., U. Schliwa, and W. Bilger. 1986. Continuous recording of photochemical and non-photochemical chlorophyll fluorescence quenching with a new type of modulation fluorometer. *Photosynth. Res.* 10:51–62.

Sebban, P., and J. C. Barbet. 1985. Simulation of the energy migration in the antenna of purple bacteria by using the Monte Carlo method. *Photobiochem. Photobiophys.* 9:167–175.

Sonneveld, A., H. Rademaker, and L. N. M. Duysens. 1979. Chlorophyll a fluorescence as a monitor of nanosecond reduction of the photooxidized primary donor P-680$^+$ of photosystem II. *Biochim. Biophys. Acta.* 548: 536–551.

Sorokin, E. M. 1971. *Fiziol. Rast. (Sofia).* 18:874–886 (in Russian).

Thielen, A. P. G. M., and H. J. van Gorkom. 1981. Energy transfer and quantum yield in photosystem II. *Biochim. Biophys. Acta.* 637:439–446.

Timpmann, K., F. G. Zhang, A. Freiberg, and V. Sundström. 1993. Detrapping of excitation energy from the reaction centre in the photosynthetic purple bacterium *Rhodospirillum rubrum*. *Biochim. Biophys. Acta.* 1183:185–193.

Trissl, H.-W., J. Breton, J. Deprez, and W. Leibl. 1987. Primary electrogenic reactions of photosystem II as probed by the light-gradient method. *Biochim. Biophys. Acta.* 893:305–319.

Trissl, H.-W. 1993. Long-wavelength absorbing antenna pigments and heterogeneous absorption bands concentrate excitons and increase absorption cross section. *Photosynth. Res.* 35:247–263.

Trissl, H.-W., Y. Gao, and K. Wulf. 1993. Theoretical fluorescence induction curves derived from coupled differential equations describing the primary photochemistry of photosystem II by an exciton/radical pair equilibrium. *Biophys. J.* 64:984–998.

Trissl, H.-W., and J. Lavergne. 1995. Fluorescence induction from Photosystem II: analytical equations for the yields of photochemistry and fluorescence derived from analysis of a model including exciton-radical pair equilibrium and restricted energy transfer between units. *Aust. J. Plant Physiol.* (in press).

van Gorkom, H. J. 1985. Electron transfer in photosystem II. *Photosynth. Res.* 6:97–112.

van Gorkom, H. J. 1986. Fluorescence measurements in the study of photosystem II electron transport. *In* Light Emission by Plants and Bacteria. X. Govindjee, J. Amesz, and D. C. Fork, editors. Academic Press, Orlando. 267–289.

Volk, M., M. Gilbert, G. Rousseau, M. Richter, A. Ogrodnik, and M. E. Michel-Beyerle. 1994. Similarity of primary radical pair recombination in photosystem II and bacterial reaction centers. *FEBS Lett.* 336:357–362.

Vredenberg W. J., and L. N. M. Duysens. 1963. Transfer of energy from bacteriochlorophyll to a reaction centre during bacterial photosynthesis. *Nature (London).* 197:355–357.

Woodbury N. W. T., and W. W. Parson. 1994. Nanosecond fluorescence from isolated photosynthetic reaction centers of *Rhodopseudomonas sphaeroides*. *Biochim. Biophys. Acta.* 767:345–361.

Woodbury, N. W., J. M. Peloquin, R. G. Alden, X. Lin, S. Lin, A. K. W. Taguchi, J. A. C. Williams, and J. P. Allen. 1994. Relationship between thermodynamics and mechanism during photoinduced charge separation in reaction centers from *Rhodobacter sphaeroides*. *Biochemistry.* 33, 8101–8112.

Wolff, C., and H. T. Witt. 1969. On metastable states of carotenoids in primary events of photosynthesis. *Z. Naturforsch.* 24b:1031–1037.

Wulf, K., and H.-W. Trissl. 1995. Fast photovoltage measurements in photosynthesis: I. Theory and data evaluation. *Biospectroscopy.* (in press).

Xiao, W. H., S. Lin, A. K. W. Taguchi, and N. W. Woodbury. 1994. Femtosecond pump-probe analysis of energy and electron transfer in photosynthetic membranes of *Rhodobacter capsulatus*. *Biochemistry.* 33:8313–8322.